A Basic Course on Accelerators for High Energy Physicists

Andreas Morsch
CERN, Geneva

June 23, 2000

1 Introduction

Accelerator physics is an interdisciplinary, applied science. Its progress has been mainly driven by the demands of high energy physics, i.e. ever higher particle energies and beam intensities. The development was guided by the knowledge on general physics but the actual design, construction, operation and exploitation of accelerators relies on many engineering techniques such as computation, magnets, power supply, vacuum and radio frequency. Accelerators have found their applications outside high energy physics. For example, in hospitals for cancer therapy, in solid state physics (neutron spectroscopy), industry (ion implantation), biology (structure analysis with synchrotron radiation). Furthermore, in the close future accelerators may play an important role in energy production and nuclear waste transmutation.

Why do we need accelerators for particle physics ? In chemical reactions density and temperature control the reaction rate. Energies in the order of some eV are needed to break up existing chemical bounds. The energy in the form of heat is distributed over many degrees of freedom.

In nuclear and elementary particle reactions, however, we need high center of mass energies, $\sqrt{s}$ in the range of 1 MeV to more than TeV in order to produce new particles or to resolve smaller and smaller structures. In the first case, the center of mass energy has to be equal or larger than the particle mass and in the latter, the minimum resolvable dimension d is related to the center of mass energy through $d = 0.2\,\mathrm{fm}/\sqrt{s}\,[\mathrm{GeV}]$.

Examples:

1. To produce a Z boson pair one needs a center of mass energy which equals at least twice the Z mass or 182 GeV. The LEP collider which today

performs electron positron collisions at a $\sqrt{s}$ close to the Z mass will be upgraded to that energy (LEP 200).

2. The HERA collider performs electron proton collisions at $\sqrt{s} = 310\,\mathrm{GeV}$. The smallest object size which can be resolved in the proton is in the order of $10^{-18}\,\mathrm{m}$.

On the other hand, we need high densities of reacting particles (Luminosity). The reaction cross-sections of point like objects falls like $1/s$. In order to maintain an equally effective physics program the luminosity has to rise at least proportional to E^2 as the energy E of the particle accelerators increases.

The broad and fast developing field of physics and engineering of accelerators and storage rings cannot be covered by a short series of lectures. Instead, it is my goal to highlight some of those aspects which are directly related to the work of a HEP experimentalist as a user in the interaction region of an accelerator or storage ring. For further reading and studies I recommend for example the proceedings of the CERN Accelerator School (CAS) [1] and the book *'The Principles of of Circular Accelerators and Storage Rings'* written P.J. Bryant and K. Johnson [2].

In the next chapter, I will give a brief overview of the development of accelerators. The linear model of transverse beam dynamics is described in the third chapter. After this lecture you will understand the terms *transfer matrix*, *alternate gradient focusing*, *β-function* and *emittance*. Using the *linear tracking* formalism we will show how the machine optics can be used to observe small scattering angles. In the forth chapter, we will see how perturbations can be treated in the linear model and you will understand *dispersion* and beam instabilities due to *resonances*. Furthermore, we will show that the dispersion of a machine can be used to measure small momentum deviations. Longitudinal beam dynamics is shortly treated in chapter 5 to explain *phase stability* and *longitudinal emittance*. An important parameter of the performance of a machine is the *luminosity* since it determines the event rate which can be observed. In chapter 6, you learn how to calculate the luminosity from the beam parameters and the *'Van der Meer' Method* for measuring the luminosity is explained.

References

[1] Proceedings of the CERN Accelerator Schools, 1985-, Editors: P. Bryant, S. Turner

[2] P.J. Bryant and K. Johnson, 'The Principles of Circular Accelerators and Storage Rings', Cambridge University Press (1992).

2 Particle Accelerators: A Brief Overview

This chapter sketches only a line through the history of accelerators and is by no means complete. Much more details can be found in the book of M.S. Livingston [1] and in a autobiographical account of R. Wideröe's life and work [2]; also the CAS lectures of K.O. Nielson [3] and P. Bryant [4] have been used to prepare this manuscript.

Electrostatic Accelerators

The simplest particle accelerators use electrostatic potentials. In the rectifier generator shown in Fig. 1, the voltage of a cascade DC generator is used to build up a potential difference between the particle source and the ground terminal. The apparatus constructed by Cockcroft and Walton 1932 [5] reaches 700 kV. They split Li nuclei with 500 keV protons, the first important nuclear physics result obtained with a particle accelerator. Sparking limits the voltage of these generators to about 1 MV, but they are still used for injection because of the high currents they can deliver.

Van de Graaf [6] placed the high voltage unit and the accelerator tube in a tank of compresses gas to rise the sparking limit and replaced the cascade generator by a charging belt (Fig. 2). The charge produced at the spray comb is transported by the belt to the top terminal. With the Van de Graaf Generator one obtains stable voltages in the range of 1 to 10 MV where saturation sets in. It can deliver beams of ions or electrons with a small momentum spread.

Linear RF Accelerator

As mentioned above, electrostatic accelerators are limited to $\sim 25\,\mathrm{MeV}$ for protons. In order to obtain higher energies one has to employ a succession of accelerating kicks to the particles. This is possible by timing bunches of particles such that they are in phase with a high frequency (RF) electro-magnetic field. In linear RF accelerators (LINAC) the accelerating elements are ordered in a linear structure.

The Wideröe type LINAC [7] shown in Fig. 3 consists of a sequence of drift tubes and gaps. Alternate tubes are connected to the same terminal of a RF generator. In order to obtain continuous acceleration the dimensions of the drift tubes have to be chosen in such a way that the electrical field vector is parallel to the particle motion when the particle is in the gap and opposite when in it is shielded by the drift tubes. The length L of the tubes has to increase proportionally to the particle velocity v. The *resonance condition* is $L = v/(2f)$, where f is the frequency of the RF source.

When the particle velocity is close to the velocity of light (relativistic particles) an energy increase results only in a small velocity increase. In this case, a traveling wave, for example the TM_{010} mode of a cylindrical tube, can be used

for acceleration. The principle can be understood by imagining the particle 'riding' the crest of the electro-magnetic wave. The phase velocity of the TM mode is, however, higher than the velocity of light. The remedy is to use an iris-loaded structure (Fig. 4) which decreases the phase velocity. Field gradients of about 30 MV are realized in machines now used for medical purposes. For the RF transmitters with frequencies between 300 and several thousand MHz are used.

The Cyclotron

LINACs are relatively complicated and expensive devices. It was soon realized that the resonance condition can be equally applied to a set-up where a magnetic field forces the particles on a circular trajectory passing the same acceleration gap several times. This principle is employed in a device called *Cyclotron* (Fig. 5), which was built for the first time 1932 by Lawrence [8]. For non relativistic particles the resonance condition is simple: the RF frequency has to be equal to the revolution frequency. For a fixed frequency the energy limit is $\sim 25\,\mathrm{MeV}$ for protons. Cyclotrons became the working tool of nuclear physics especially because of the high number (*intensity*) of particles that could be accelerated.

For relativistic energies the revolution frequency decreases with rising energy. Hence, the RF frequency has to be down-modulated in order to maintain the resonance condition. The highest energy obtained with such a *synchro-cyclotron* is 720 MeV at the Berkeley 184 inch. With synchro-Cyclotrons one could systematically investigate artificially produced mesons and the era of particle physics started.

For an accelerator it is not only important to cope with a resonance condition but the motion of the particles also has to be stable against all kinds of imperfections as for example the natural divergence of the injected beam and its momentum spread and and all kinds of asymmetries in the magnetic fields. If the beam is not stable a large fraction of the particles can be lost during acceleration and the currents are too low for performing experiments. It is therefore important to introduce focusing elements into the accelerator.

Because of the momentum spread different particles have different resonance frequencies. It was shown by McMillan and Veksler [10], [11] that a stable motion of all particles can be obtained if the particles have a certain phase difference with respect to the RF (*principle of phase stability*). The principle is illustrated in Fig. 6. Here, particles which are slower than exactly synchronous particles arrive later in phase and get a stronger kick from the RF field. Conversely, faster particles arrive earlier and get a weaker kick. In both cases the phase swings in the direction of the nominal phase. Actually, all particles execute so called *synchrotron oscillations* about the nominal phase.

The Betatron

Because of their small mass (1/2000 of the proton mass) electrons become relativistic at very low energies and Cyclotrons can not be used as electron accelerators. An accelerator adapted for electrons is the betatron [9] or 'beam transformer' as it was called by Wideröe [7]. The principle of this device is shown in Fig. 7. As in the cyclotron the electron is kept by a magnetic field on a circular orbit. Acceleration is achieved by increasing the magnetic field: the time-varying magnetic field perpendicular to the plane of motion induces an electrical field parallel to the particle direction. It was shown by Wideröe that in order to keep the electrons on a circle with constant radius the magnetic field strength averaged over the area of the circle has to increase at twice the rate as the magnetic 'guide' field at the radius of the particle. With a betatron electrons can be accelerated up to 200 MeV. It is a robust device frequently used in hospitals for cancer therapy.

Synchrotrons

As the betatron the synchrotron uses a magnetic bending field which increases during acceleration to keep the particles on a circular orbit [10], [11] . Acceleration is by a RF voltage operated at the revolution frequency or a higher harmonic. The frequency has to be upward-modulated synchronously as the velocity of the particle increases. The first Synchrotron built was the Cosmotron (1952), a 3 GeV proton accelerator (Fig. 8).

Weak and Strong Focusing

In order to maintain transverse stability all accelerators built before 1952 used so called weak focusing magnets. The magnetic field of the bending magnets decreases slightly in the vicinity of the nominal orbit. Particles perform stable motions, so called *betatron oscillations*, about the nominal orbit. The amplitude of these oscillations depends on the focusing power of the system. Hence, the aperture needed to contain the beam in a 'weakly focusing' accelerator is large and the magnets become very costly for big machines limiting the maximum energy to about 10 GeV.

The concept of strong focusing can be understood from the fact that a pair of optical focusing and defocusing lenses can be arranged in such a way that the total system is focusing. Magnetic quadrupoles act for charged particles as optical lenses. Christofilos and independently Courant, Livingston and Snyder [12] showed that certain arrangements of quadrupoles with *alternating magnetic gradients (AG)* (Fig. 9) can be used to achieve a stable particle motion. The focusing power of the AG system is much stronger than that of weakly focusing magnets and the way was now open to built accelerators with energies three orders of magnitude higher than could have been envisaged with the old technology.

Colliders

As pointed out in the introduction, for high energy physics the important quantity of an accelerator experiment is the center of mass energy of the colliding particles. All experiments before 1962 where so called 'fixed target experiments' where the accelerated particles collide with a target at rest. The advantage of fixed target experiments is that one can provide a variety of secondary beams of hadrons (p, K, p, π ...) and leptons (e, μ, ν ...) and that the reaction rate is high. Its big disadvantage is, however, the waste of energy.

In the fixed target scenario, the center of mass energy is given by the expression:

$$\sqrt{s} = \sqrt{2m_p E}\,, \tag{1}$$

where m_p is the proton mass and E the energy of the projectile particle. It is evident that only a fraction of the energy can be used for the particle reaction. This fraction decreases with increasing particle energy:

$$\frac{\sqrt{s}}{E} \propto \frac{1}{\sqrt{E}} \tag{2}$$

In colliding beam accelerators, generally, two particles of the same mass and energy collide head-on. In this case, the center of mass energy is twice the particle energy. The first machines of this kind where the 2x200 MeV electron positron collider, Anelli di Accumulazione (AdA) at Frascati and the 2x500 MeV Princeton Standford collider. Since they have opposite charge, electrons and positrons can be accelerated in the same ring (*single ring colliders).*

Electron positron colliders dominated high energy physics in the sixties and seventies. The largest e^+e^- machine is the LEP at CERN, Geneva, which started operation in 1989 and operates currently at a energy up to 2x55 GeV. It will be upgraded to 2x100 GeV which is the limit set by the inherent energy loss through synchrotron radiation. Future electron positron colliders with higher energy have to be linear colliders. The principle is successfully tested at the 2x50 GeV Standford Linear Collider (SLC) [14] which started operation in the same year as LEP.

Single ring proton anti-proton colliders can not be built in the same way as e^+e^- colliders. The reason is that anti-proton sources have a much too low intensity to cope with the required luminosities. Thus, the first colliding beam facility for protons was a double ring collider the 2x31 GeV Intersection Storage Ring (ISR) [13] at CERN. The ISR started operation in 1971. Until its shut-down in 1984 its performance was steadily improved creating a general confidence in the predictability of hadron colliders.

A next big step in the direction of higher energies was possible through the invention of *stochastic cooling* by Simon van der Meer [15] with which it was possible to reduce the beam dimension of an anti-proton beam and thus increase

its intensity. The technique was adopted by C. Rubbia *et al.* [16] in their project to accumulate and cool low energetic antiprotons in a storage ring over a long period then accelerating them in the existing CERN Super Proton Synchrotron SPS up to 270 GeV and collide them with a proton beam. With the discovery of the intermediate vector bosons W and Z the facility (Sp$\bar{\text{p}}$S) had a spectacular success. A similar accelerator complex the TeVATRON [17] started operation in 1985 at Fermilab, Chicago. It now operates at a energy of 2x900 GeV. The two experiments at the Fermilab collider, CDF and D0, observe significant signals of the heaviest lepton of the standard model, the top quark.

An important new feature of the TeVATRON is the use of *super conducting magnets*. The advantage of super conducting magnets is the high field strength (up to 8 T) that can be reached keeping the size and hence the cost of the collider small as compared to conventional technology (up to 1.5 T).

A different kind of machine is HERA [18] at DESY (Hamburg). It is a double ring collider shooting electrons on protons at a $\sqrt{s}$ of 310 GeV. The collider acts like a huge *electron microscope* exploring the proton structure down to 10^{-18} m.

Accelerator Complexes

Modern accelerator facilities as at CERN or Fermilab provide complexes of linked injectors, accumulators, accelerators and storage rings. Fig. 10 shows a part of the CERN accelerator complex including the SPS. In future the SPS will inject protons in a even larger machine, the LHC [19], which will be accommodated in the existing LEP tunnel. At LHC, one will perform proton proton collisions at a center of mass energy of 14 TeV and one hopes to observe the yet undiscovered Higgs boson.

References

[1] M.S. Livingston, 'Particle Accelerators: A Brief History', Harvard Univ. Press, Cambridge, Masachusetts (1969).

[2] 'The Infancy of Particle Accelerators - Life and Work of Rolf Wideröe', Compiled and Edited by P. Waloschek, DESY 94-039 (1994).

[3] K.O. Nielson, 'Historical Introduction and Present Day Accelerators', Proceedings of the CAS, Gif-sur-Yvette, Paris, (1985), Editors: P. Bryant, S. Turner.

[4] P. Bryant, 'A Brief History and Review of Accelerators', Proceedings of the CAS, Univ. of Jyvaskyla, Finland (1985), Editor: S. Turner.

[5] J.D. Cockcroft and E.T.S. Walton, Proc. Royal Soc., **A136** (1932) 619-30.

[6] R.J. Van de Graaff, Phys. Rev. **387** (1931) 1919-20.

[7] R. Wideröe, Arch. fur Elektrotechnik (Berlin) **21** (1928) 387-406.

[8] E.O. Lawrence and N.E. Edlefsen, Science **72** (1930) 376-7.

[9] D.W. Kerst, Phys. Rev. **60** (1942) 47-53.

[10] E.M. McMillan,Phys. Rev. Lett. to the Editor **68** (1945) 1434.

[11] V. Veksler, J. of Phys., USSR **9** (1945) 413.

[12] E.D. Courant, M.S. Livingston and H.S. Snyder, Phys. Rev. **88** (1952) 1190-6.
E.D. Courant and H.S. Snyder, Annals of Physics **3** (1958) 1-48.

[13] M. Jacob and K. Johnsen, CERN/LEP 84-13 (1984).

[14] J. Seeman, Annu. Rev. Nucl. Part. Sci. **41** (1991) 389-428.

[15] S. van der Meer, CERN/ISR-PO/72-31 (1972),
P. Bramham *et al.* , Nucl. Instr. Methods **125** (1975) 201.

[16] C. Rubbia *et al.* , Proc. of the International Neutrino Conference, Aachen (1976).

[17] F. Abe *et al.* , Fermilab Preprint PUB-95-022-E,
S. Abachi *et al.* , Fermilab Preprint PUB-95-028-E.

[18] DESY HERA 81-10 (1981).

[19] The LHC Study Group, CERN/AC/93-03 (LHC).

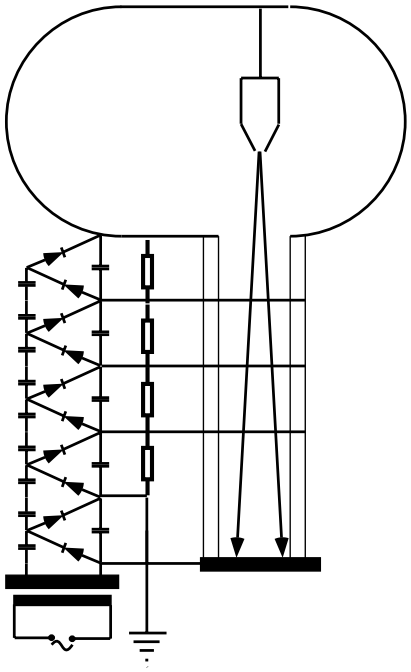

Figure 1: *Cascade DC Generator*

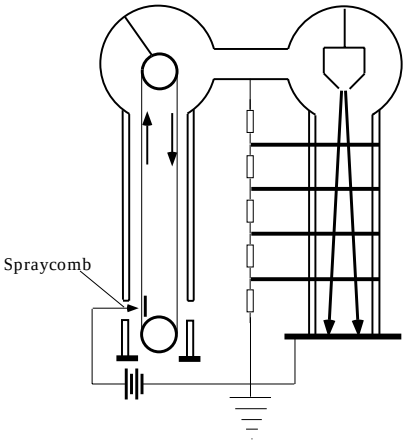

Figure 2: *Van de Graaf Generator*

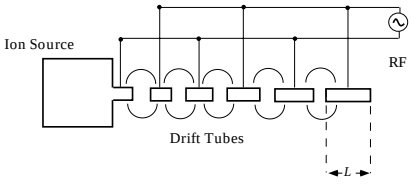

Figure 3: *Wideröe-Type LINAC*

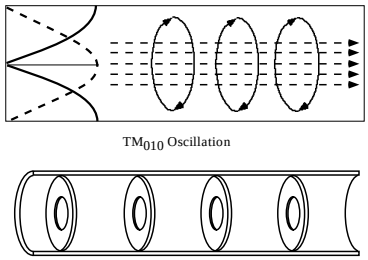

Figure 4: $TM_0 10$ *Mode and Iris Loaded Structure*

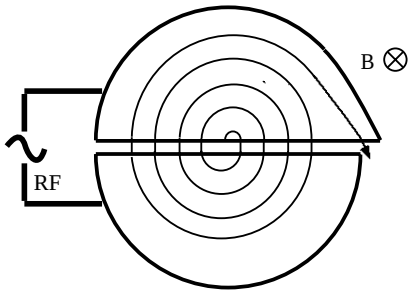

Figure 5: *Cyclotron*

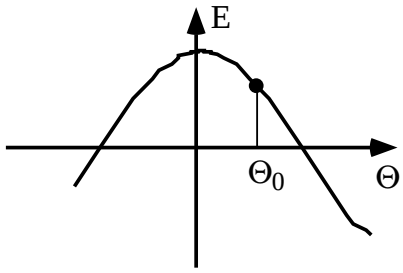

Figure 6: *Phase Stability*

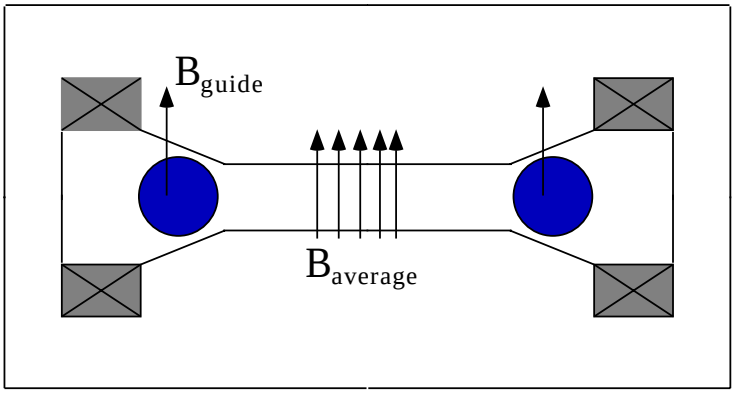

Figure 7: *Betatron*

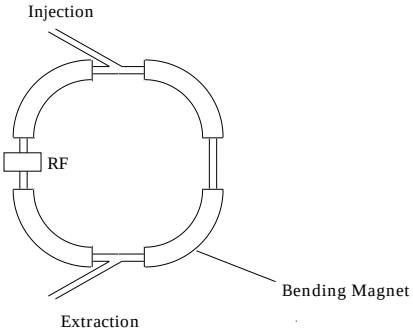

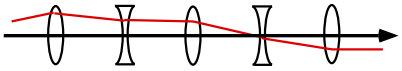

Figure 9: *Strong Focusing*

Figure 8: *Synchrotron*

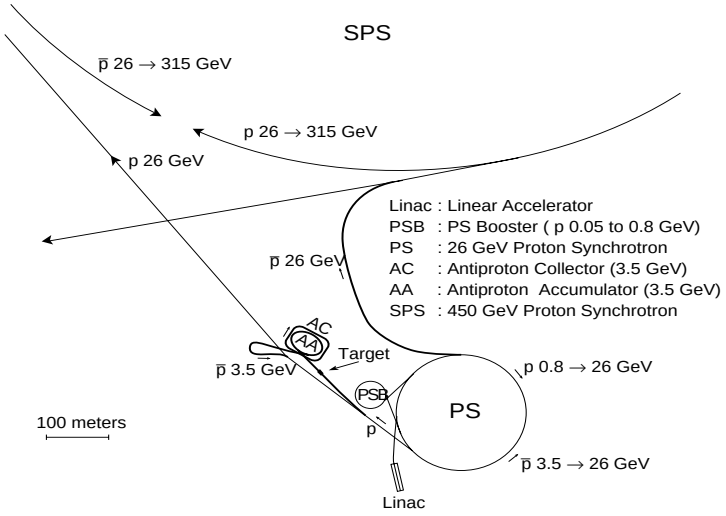

Figure 10: *CERN SppS*

3 Transverse Particle Motion in a Circular Storage Ring

Ideally, particles in a circular storage ring move along straight lines when they are in a drifts-pace and along circle segments when they traverse a dipole magnet. The nominal orbit closes after one turn and approximates in its shape a circle. In real life, however, the particles do not have the same initial conditions when they arrive at the storage ring: they have different angles, positions and momenta with respect to the nominal particle.

A storage ring consisting only of straight sections and dipoles has an inherent problem: a *rms* angular spread $\Delta\theta$ of the beam particles transforms after a quarter turn into a spatial spread of $\rho\Delta\theta$, where ρ is the radius of the machine. An angular spread of some mrad, for example, would result in a beam width of some meters if the radius is in the order of km. This would require magnet dimensions which make the machine un-payable. The remedy is to use quadrupole magnets introducing a restoring force proportional to the excursion of the particle.

In the following section we will write down the general equations of motion of a charged particle in a magnetic field. This equations are inherently non linear and one can not learn much from them. If we consider, however, deviations from the nominal orbit that are much smaller than the bending radius and allow only magnetic dipole and quadrupole fields the equation of motion can be linearized. Many important features of transverse beam dynamics can be understood within this linear model. More details may be found in references [1] - [5], which have also been used for the preparation of this lecture.

3.1 The Equation of Motion and its Linearisation

The equation of motion of a charged particle in a magnetic field $\vec{B}$ using Cartesian coordinates is:

$$\frac{dp}{dt} = \frac{d}{dt}(m\vec{v}) = -e(\vec{v} \times \vec{B}) \tag{1}$$

Rewriting the equation for cylindrical coordinates $(\rho\,, \theta\,, z)$ defined in Fig. 1 one obtains:

$$F_\rho = \frac{d}{dt}(m\dot{\rho}) - m\rho\dot{\theta}^2 = -e\rho\dot{\theta}B_z \tag{2}$$

$$F_\theta = \frac{1}{\rho}\frac{d}{dt}(m\rho^2\dot{\theta}) = -e(\dot{z}B_r - \dot{\rho}B_z) \tag{3}$$

$$F_z = \frac{d}{dt}(m\dot{z}) = e\rho\dot{\theta}B_r \tag{4}$$

In case of a circular motion in a constant dipole field B_0 with radius

$$\rho = \rho_0 = \text{const.} \tag{5}$$

one obtains for the relation between momentum p, radius and magnetic field strength the *cyclotron relation*:

$$\frac{p}{e} = B_0 \rho_0 \,,$$

which gives in practical units:

$$B\,[\mathrm{T}]\rho\,[\mathrm{m}] = 3.3356\,p\,[\mathrm{GeV/c}]\,. \tag{6}$$

Furthermore, the angular velocity is independent of the bending radius:

$$\dot{\theta} = \frac{e}{m} B_0 = \Omega_c\,. \tag{7}$$

Example:
The bending radius of a 7000 GeV proton in a magnetic field of 8 T amounts to 2.9 km.

Assuming that the deviations from a circular orbit are small the azimuthal component of the particle velocity $v_\theta = r\dot{\theta}$ is much larger than the transverse components v_r and v_z so that:

$$\dot{\theta} \simeq \frac{v}{\rho(t)}\,. \tag{8}$$

In this case the radial magnetic force looks like a central force balanced by the radial acceleration:

$$F_\rho = \frac{d}{dt}[m\dot{\rho}] - \frac{mv^2}{\rho} = -evB_z\,. \tag{9}$$

In the next steps we replace the time t by the distance s measured along the beam trajectory:

$$\frac{d}{dt} \equiv v\frac{d}{ds} \tag{10}$$

and for the magnetic field we consider only the first two terms of a Taylor expansion corresponding to dipole and quadrupole field components:

$$\Delta B_z = B_z - B_0 = \left[\frac{\partial B_z}{\partial x}\right]_0 x + \ldots \tag{11}$$

For the quadruple component we define the focusing strength k as the normalized field gradient:

$$k = -\frac{1}{B_0 p_0}\left[\frac{\partial B_z}{\partial x}\right]_0\,. \tag{12}$$

The radial coordinate ρ can be replaced by the excursion x which measures the radial deviation of the particle from the nominal orbit:

$$x = \rho - \rho_0 \ . \tag{13}$$

Under the assumption that the excursion is small against the local radius of gyration ($x \ll \rho_0$) one obtains:

$$\frac{d^2}{ds^2}x + \frac{1}{\rho_0}\frac{p_0}{p} - \frac{1}{\rho} - kx = 0 \tag{14}$$

Assuming small momentum deviations Δp and excursions x we can write

$$\frac{p_0}{p} = 1 - \frac{\Delta p}{p_0} \tag{15}$$

$$\frac{1}{\rho} = \frac{1}{\rho_0}\left(1 - \frac{x}{\rho_0}\right) \tag{16}$$

and it follows the linearized equation of motion:

$$x'' - \left(k - \frac{1}{\rho_0^2}\right)x = \frac{1}{\rho_0}\frac{\Delta p}{p_0} \tag{17}$$

The motion in the z-direction (perpendicular to the bending plane) can be derived in an analogous way. Note that since $\nabla \times \vec{B} = 0$ the field gradients are related by

$$\begin{gathered}\frac{\partial B_x}{\partial z} = -\frac{\partial B_z}{\partial x} \\ k \to -k\end{gathered} \tag{18}$$

The equations of motion for small particle excursions in the z-direction is:

$$z'' + kz = 0. \tag{19}$$

The term $1/\rho_0^2$ in equ. (17) describes the weak focusing of a pure bending magnet. For accelerators with large radius, it can be neglected compared to the strong quadruple focusing k.

Examples:
The HERA proton ring has $k = 0.032\,\mathrm{m}^{-2}$ and $1/\rho^2 = 2.9\,10^{-6}\,\mathrm{m}^{-2}$. The LHC will have $k = 0.093\,10^{-2}\,\mathrm{m}^{-2}$ and $1/\rho^2 = 1.1\,10^{-7}\,\mathrm{m}^{-2}$.

In the following, we will discuss the solutions of the equation of motion for the special case where $k(s) = const.$ and $\Delta p = 0$. The equation of transverse motion without momentum deviation can be written in the more general form:

$$x''(s) + K(s)x(s) = 0\,, \tag{20}$$

where $K(s)$ is 0 for a drift space, $1/\rho^2$ for a bending magnet and k $(-k)$ for a focusing (defocusing) quadrupole. Within these elements $K(s)$ is constant and well known solutions exist for these intervals in s:

$$x(s) = \begin{cases} x_0 \cos\sqrt{k}s + \frac{x_0'}{\sqrt{k}} \sin\sqrt{k}s & \text{if } K > 0, \\ x_0 + x_0' s & \text{if } K = 0, \\ x_0 \cosh\sqrt{k}s + \frac{x_0'}{\sqrt{k}} \sinh\sqrt{k}s & \text{if } K < 0\ . \end{cases} \tag{21}$$

where x_0 and x_0' are the initial conditions at for $x(s)$ and $x'(s)$ at the entrance of the element. The general solution can be written in the form :

$$x(s) = x_0 C(s) + x_0' S(s)\,. \tag{22}$$

$C(s)$ and $S(s)$ being two independent solutions, the Wronski determinant W has to meet the condition:

$$W = \begin{vmatrix} C & S \\ C' & S' \end{vmatrix} \neq 0 \tag{23}$$

This implies that the derivative of W vanishes identically:

$$\frac{dW}{ds} = \frac{d}{ds}(CS' - SC') = CS'' - SC'' = -K(CS - SC) = 0 \tag{24}$$

Hence, the value of W is determined everywhere by the initial conditions which we can choose as:

$$C_0 = 1\,, C_0' = 0\,, S_0 = 0\,, S_0' = 1 \rightsquigarrow W = 1\,. \tag{25}$$

3.2 Analogy with Ray Optics and Transfer Matrices

In Fig. 2, we illustrate for a focusing optical lens how one can construct the image of an object using two independent 'ray-vectors'. Using this ray vectors as basis vectors of a Cartesian coordinate system the action of the lens can be written as a linear transformation:

$$\begin{pmatrix} x \\ x' \end{pmatrix} = \begin{pmatrix} 1 & 0 \\ -1/f & 1 \end{pmatrix} \begin{pmatrix} x_0 \\ x_0' \end{pmatrix} \tag{26}$$

In the same way we can write the solutions for the transverse motion of particles in the elements of an accelerator optics:

$$\begin{pmatrix} x(s) \\ x'(s) \end{pmatrix} = \begin{pmatrix} C(s) & S(s) \\ C'(s) & S'(s) \end{pmatrix} \begin{pmatrix} x_0 \\ x_0' \end{pmatrix} \tag{27}$$

For each element of the machine optics $C(s)$ and $S(s)$ are constants. The solution for a string of elements can be obtained by multiplying subsequently with the transfer matrix of each element:

$$\vec{x}(s) = M\vec{x}_0 = M_N \bullet M_{N-1} \ldots \bullet M_1 \vec{x}_0 \tag{28}$$

The simplest transfer matrix is that of a drift space of length l. The matrices for the x and z directions are equal:

$$M_{x,z} = \begin{pmatrix} 1 & l \\ 0 & 1 \end{pmatrix} \tag{29}$$

For the sector dipole magnet shown in Fig.3 the transfer matrices are:

$$M_x = \begin{pmatrix} \cos\varphi & \rho\sin\varphi \\ -1/\rho\sin\varphi & \cos\varphi \end{pmatrix}, \quad M_z = \begin{pmatrix} 1 & l \\ 0 & 1 \end{pmatrix}, \tag{30}$$

where the length l. The bending radius ρ and the bending angle φ are related through:

$$\varphi = l/\rho \tag{31}$$

For small bending angles one can use the approximation:

$$M_x = \begin{pmatrix} 1 & l \\ -l/\rho^2 & 1 \end{pmatrix}. \tag{32}$$

Comparing with the transfer matrix of a thin lens we see that a sector magnet acts in the x-direction like a focusing lens and in the z-direction like a drift space.

The transfer matrices for a quadrupole which focuses in the x-direction are:

$$M_x = \begin{pmatrix} \cos\varphi & 1/\sqrt{k}\sin\varphi \\ -\sqrt{k}\sin\varphi & \cos\varphi \end{pmatrix} \tag{33}$$

$$M_z = \begin{pmatrix} \cosh\varphi & 1/\sqrt{k}\sinh\varphi \\ \sqrt{k}\sinh\varphi & \cosh\varphi \end{pmatrix}, \tag{34}$$

where $\varphi = l\sqrt{k}$. For the thin lens approximation

$$l\sqrt{k} \ll 1 \tag{35}$$

one obtains with $1/f = l\sqrt{k}$:

$$M_x = \begin{pmatrix} 1 & 0 \\ -1/f & 1 \end{pmatrix}, M_z = \begin{pmatrix} 1 & 0 \\ 1/f & 1 \end{pmatrix}. \tag{36}$$

The magnetic potential Φ within a quadrupole (4) is:

$$\Phi(x,z) = gxz \tag{37}$$

and the magnetic field is $\vec{B} = -\nabla\Phi = -g(z,x)$ or $\left|\vec{B}\right| = g\sqrt{x^2+z^2} = gr$. Hence, the magnetic field strength depends only on the distance r from the

axis. In practical units the relation between focusing strength k and gradient g is:

$$k[\mathrm{m}^{-2}] = 0.2998 \frac{g[\mathrm{T/m}]}{p[\mathrm{GeV/c}]} \tag{38}$$

Example:
The focusing strength of a quadrupole magnet with a gradient of 200 T/m is for 7 TeV particles $8.610^{-3}\mathrm{m}^{-2}$. Assuming a magnetic length of 5 m the focusing length amounts to 23 m.

From equ. (18) we see that a quadrupole acts always focusing in one and defocusing in the other direction. It is, however, possible to arrange a sequence of focusing and defocusing lenses in such a way that the net effect is focusing. Using the matrix formalism derived above it is easy to derive a stability criterion for the lattice.

3.3 Stability Criterion

Particles traveling through a circular storage ring see an infinite sequence of transfer matrices T, where T can be the transfer matrix for the full orbit or for a machine cell which repeats itself m-times (m=2, 3 , 4 ..). Hence, one can write for the transfer matrix of n cells:

$$\begin{pmatrix} y \\ y' \end{pmatrix}_n = T^n \begin{pmatrix} y \\ y' \end{pmatrix}_0 . \tag{39}$$

In order to maintain a stable motion T_n must stay finite. Consider the eigenvalues λ_1 and λ_2 of T defined by the equation:

$$T y_{1,2} = \lambda_{1,2} y_{1,2} \tag{40}$$

or

$$\det T - \lambda I = 0 . \tag{41}$$

Writing T in the form

$$T = \begin{pmatrix} a & b \\ c & d \end{pmatrix} \tag{42}$$

yields

$$\lambda^2 - \lambda \underbrace{(a+d)}_{\mathrm{traceT}} + \underbrace{(ad-bc)}_{1} = 0 \tag{43}$$

$$\lambda^2 - \lambda \mathrm{trace} T + 1 = 0 . \tag{44}$$

Introducing a new parameter $\cos\mu$

$$\cos\mu = \frac{1}{2}\mathrm{trace}T \tag{45}$$

the eigenvalues are:

$$\lambda_{1,2} = \cos\mu \pm \imath \sin\mu = \exp \pm \imath\mu \; . \tag{46}$$

Now we can re-express T^n using a similarity transformation S and one obtains:

$$T^n = S \begin{pmatrix} e^{+\imath\mu} & 0 \\ 0 & e^{-\imath\mu} \end{pmatrix}^n S^{-1} = S \begin{pmatrix} e^{+\imath n\mu} & 0 \\ 0 & e^{-\imath n\mu} \end{pmatrix} S^{-1} \, . \tag{47}$$

The particle excursions stay finite if μ is real and we arrive at the stability condition for a circular storage ring:

$$\frac{|\mathrm{trace}T|}{2} < 1 \, . \tag{48}$$

Example: FODO Cell

The simplest sequence of strongly focusing elements leading to a stable motion is the so called FODO cell consisting of a focusing (f_1) and a defocusing quadrupole (f_2) separated by a drift space of length L. In the thin lens approximation the transfer matrix in x-direction is:

$$T_x = \begin{pmatrix} 1 & L \\ 0 & 1 \end{pmatrix} \begin{pmatrix} 1 & 0 \\ 1/f_2 & 1 \end{pmatrix} \begin{pmatrix} 1 & L \\ 0 & 1 \end{pmatrix} \begin{pmatrix} 1 & 0 \\ 1/f_1 & 1 \end{pmatrix} \tag{49}$$

Evaluating the trace of the matrix one obtains the stability condition:

$$\frac{|\mathrm{trace}T_x|}{2} = \left|1 + L/f_1 + L/f_2 + L^2/(2f_1f_2)\right| < 1$$

Evaluating the expression writing $d_1 = L/f_1$ and $d_2 = L/f_2$

$$d_2 < \frac{-d_1}{1 - 0.5(-d_1)} \wedge -d_1 < 2 \tag{50}$$

and similarly for the z-direction:

$$-d_1 < \frac{d_2}{1 - 0.5d_2} \wedge d_2 < 2 \tag{51}$$

Plotting the condition in the $(-d_1) - d_2$ plane one obtains the diagram shown in Fig. 5. The region of stability looks like a necktie (*Necktie Diagram*).

3.4 Parameterization of the Transverse Motion

So far we obtain a stepwise solution of the transverse particle motion by multiplication of a transfer matrix for each element the particle traverses. This procedure is, however, somewhat unsatisfactory, because of the lack of a smooth trajectory. Furthermore, we do not make use of the pseudo harmonic appearance of the equation of motion and the machine periodicity. Finally, it is difficult to imagine how one could treat perturbations of the ideal motion.

The equation of motion

$$\frac{d^2y}{ds^2} + K(s)y = 0 \tag{52}$$

corresponds for $k = const > 0$ to a harmonic oscillator with the solution

$$y(s) = C\cos\left(\sqrt{K}s + \mu_0\right). \tag{53}$$

For the general solution we can try the pseudo-harmonic ansatz by varying the constants:

$$y(s) = A\sqrt{\beta(s)}\cos\left(\mu(s) + \mu_0\right). \tag{54}$$

Inserting the new variable β, the *betatron amplitude function*, in the equation of motion one obtains the diff. equation:

$$\frac{d^2}{ds^2}\beta^{\frac{1}{2}} + K(s)\beta^{\frac{1}{2}} = \beta^{-\frac{3}{2}}\,. \tag{55}$$

Furthermore, the phase advance $\mu(s)$ is related to the β-function through

$$\mu(s) = \int_0^s \frac{d\sigma}{\beta(\sigma)}\,. \tag{56}$$

The solution for the particle excursion can be written in the form

$$\begin{aligned} y(s) &= C\beta^{\frac{1}{2}}\cos\left(\mu + \mu_0\right) \\ &= A\beta^{\frac{1}{2}}\cos\mu + B\beta^{\frac{1}{2}}\sin\mu\,. \end{aligned} \tag{57}$$

Introducing a new variable α for the derivative of β.

$$\alpha(s) = -\frac{1}{2}\frac{d}{ds}\beta(s) \tag{58}$$

one can write for the $y(s)$ and its derivative $y'(s)$:

$$\begin{pmatrix} y(s) \\ y'(s) \end{pmatrix} = \begin{pmatrix} \beta^{1/2}\cos\mu & \beta^{1/2}\sin\mu \\ -\beta^{1/2}(\alpha\cos\mu + \sin\mu) & \beta^{-1/2}(\cos\mu - \alpha\sin\mu) \end{pmatrix} \begin{pmatrix} A \\ B \end{pmatrix} \tag{59}$$

Inserting the initial conditions (y_0, y_0') at $s = s_0$ one obtains for A and B:

$$A = y_0\beta_0^{-1/2} \tag{60}$$
$$B = y_0'\beta_0^{1/2} + y_0\alpha_0\beta_0^{-1/2} \tag{61}$$

The solution may now be written as the product of a generalized transfer matrix $T(s|s_0)$ and the initial conditions:

$$\begin{pmatrix} y(s) \\ y'(s) \end{pmatrix} = T(s|s_0)\begin{pmatrix} y(s_0) \\ y'(s_0) \end{pmatrix}, \tag{62}$$

where $\Delta\mu$ denotes the phase difference between the two positions. Now we make use of the fact that the focusing function has a periodicity:

$$K(s) = K(s + L), \tag{63}$$

Imposing the condition

$$\beta_1 = \beta_2 = \beta \tag{64}$$
$$\alpha_1 = \alpha_2 = \alpha \tag{65}$$

for $s_2 = s_1 + L$ we obtain for the transfer matrix of one period:

$$\begin{aligned} T(s + L|s) &= \begin{pmatrix} \cos\mu_0 + \alpha\sin\mu_0 & \beta\sin\mu_0 \\ -\gamma\sin\mu_0 & \cos\mu_0 - \alpha\sin\mu_0 \end{pmatrix} \\ &= I\cos\mu_0 + J\sin\mu_0 \end{aligned} \tag{66}$$

with

$$I = \begin{pmatrix} 1 & 0 \\ 0 & 1 \end{pmatrix}; J = \begin{pmatrix} \alpha & \beta \\ \gamma & -\alpha \end{pmatrix} \tag{67}$$

and

$$\left\{ \begin{array}{c} \beta \\ \alpha = -\frac{1}{2}\frac{d\beta}{ds} \\ \gamma = (1 + \alpha^2)/\beta \end{array} \right\} \quad \text{Courant Snyder or Twiss Parameters} \tag{68}$$

$$\mu_0 \quad \text{Phase Advance per Revolution} \tag{69}$$

$$Q = \frac{\mu_0}{2\pi} \quad \text{Tune} \tag{70}$$

Examples:

(1) The β-function of a symmetric interaction region

Let s_0 be the position of a symmetric interaction region ($\alpha_0 \propto d\beta/ds = 0$) then the matrix $T(s|s_0)$ for transforming a particle position in phase space (y_0, y_0') to a point s along the beam line is:

$$T(s|s_0) = \begin{pmatrix} (\beta/\beta_0)^{1/2}\cos\Delta\mu & (\beta\beta_0)^{1/2}\sin\Delta\mu \\ -(\beta\beta_0)^{-1/2}\sin\Delta\mu & (\beta_0/\beta)^{1/2}\cos\Delta\mu \end{pmatrix} \tag{71}$$

Between the interaction point and the first magnetic elements their is always a drift space of length L in which the experiments are placed. For this drift space the transfer matrix is:

$$T(s|s_0) = \begin{pmatrix} 1 & L \\ 0 & 1 \end{pmatrix} \tag{72}$$

Comparing the two matrices one finds for the β-function in the drift space of a symmetric interaction region:

$$\beta(s) = \beta^\star \left(1 + \frac{s^2}{\beta^{\star 2}}\right) \tag{73}$$

where $\beta^\star$ is the value of the β-function at the interaction point.

The phase advance $\Delta\mu$ in the drift space is given by:

$$\Delta\mu = \int_{-L}^{L} \frac{1}{\beta(s)} ds = \frac{1}{\beta^\star} \int_{-L}^{L} \frac{1}{1 + s^2/\beta^\star} ds = 2 \arctan \frac{L}{\beta^\star} \tag{74}$$

In order to obtain very high luminosities it is necessary that the beam density in the interaction point is very high. We see later that in this case $\beta^\star$ has to be small. In the case $L \gg \beta^\star$ the phase advance is equal to π. Hence every high luminosity interaction region contributes with a phase advance of π to the total tune of the machine.

(2) Tracking particles emerging from a symmetric interaction region

From equ. (71) we see that a particle with a excursion $x^\star$ and the angle $x'^\star$ at the interaction point will have at a distance s from the interaction the excursion $x(s)$ given by:

$$\begin{aligned} x(s) &= (\beta/\beta^\star)^{1/2}\cos\Delta\mu x^\star + (\beta\beta^\star)^{1/2}\sin\Delta\mu x'^\star \\ &= v x^\star + L_{\text{eff}} x'^\star \\ v: &\quad \text{Magnification} \\ L_{\text{eff}}: &\quad \text{Effective Length} \end{aligned} \tag{75}$$

3.5 Phase Space Trajectories and Emittance

The equations

$$y = A\sqrt{\beta}\cos(\mu+\mu_0) \quad (76)$$

$$y' = A/\sqrt{\beta}(\sin(\mu+\mu_0)+\alpha\cos(\mu+\mu_0)) \quad (77)$$

represent a parameterization of an ellipse in the (y, y') plane (phase space plane). Fig. 6a shows the ellipses for two particles with different values of the parameter A and Fig. 6b shows as solid points the phase space positions of one and the same particle observed at a fixed position along the beam line. Note that for each revolution in the machine the particle makes Q revolutions in the phase space plane.

Eliminating the phase terms in the ellipse parameterization yields the Cartesian co-ordinate representation of the beam ellipse:

$$\gamma y^2 + 2\alpha y y' + \beta {y'}^2 = A^2 = const. \text{ (Courant Snyders Invariant)} \quad (78)$$

The area of the ellipse is $S = \pi A^2$. The form of the ellipse changes as we move along the beam axis but the area stays constant. S is also called the *single particle emittance*.

The invariance of the phase space are is a direct consequence of the Liouville Theorem which states:

In the vicinity of a particle, the particle density in phase space is constant if the particles move in an external magnetic field or in a general field in which the forces do not depend on velocity.

A particle beam consists typically of 10^{10} to 10^{13} particles each with its own invariant single particle emittance S. Imagine that one could measure at a fixed point along the beam line the position (y, y') in phase space of all particles. The projection of the positions on the $y-$axis will then give a statistical distribution of the particle excursions, which one calls *beam profile* (Fig. 7). Instead of the single particle emitttances it is convenient to define the beam emittance ϵ which is a measure for the beam density independent of the beta value:

$$\epsilon = \frac{\sigma_y^2}{\beta_y} \quad (79)$$

Up to now we did not take into account the possibility that the particles change their momenta, for example during acceleration. In this case y' and hence ϵ will not be constant anymore. Since, however, the acceleration is only parallel to the beam line, the transverse momentum p_y of each particle stays constant:

$$p_y = y'p = y'\beta\gamma m_0 = const. \Rightarrow y' \propto \frac{1}{\beta\gamma}, \quad (80)$$

where the factor $\beta\gamma$ is the ratio of the particle momentum p over its rest mass and should not be confused with the Twiss parameters. The invariant of the motion for arbitrary momentum is the phase space integral

$$\int dp_y y = const._\gamma \,, \tag{81}$$

which leads to the definition of the normalized emittance ϵ_n:

$$\epsilon_n = \beta\gamma \frac{\sigma_y^2}{\beta_y} = const._\gamma \tag{82}$$

From this relation we see that the width of the beam profile decreases during acceleration. The process is called *adiabatic damping*. Fig. 8 shows the relation between the emittance ϵ, the β-function and the beam parameters.
Examples:

1. Beam Size at the LHC

   The normalized emittance of the LHC will be $3.75\,\mu$m at $\gamma = 7463$. In the high luminosity interaction regions $\beta^\star$ amounts to 0.5 m. The beam size in the interaction point is $\sigma^\star = \sqrt{\epsilon_n \beta^\star/\gamma} = 15.8\,\mu$m and the beam divergence $\sqrt{\epsilon_n/(\beta^\star\gamma)} = 32\,\mu$rad. In the arcs, where the average value of the β-function is $\sim 100\,$m the beam size amounts to $220\,\mu$m.

2. Observation of small scattering angles.

   Particles which are scattered under a very small angle can only be observed if the excursion of the particle is a factor 10-15 larger than the beam width at the position of the detector up streams of the collision point.

   The excursion x (Fig. 9) at a distance s from the interaction point is:

   $$x(s) = \sqrt{\beta(s)\beta^\star}\sin\Delta\mu\theta^\star + \sqrt{\beta(s)/\beta^\star}\cos\Delta\mu x^\star \,, \tag{83}$$

   where $\theta^\star$ is the scattering angle and $x^\star$ the transverse position of the collision. Choosing $\Delta\mu$ close to $\pi/2$ the excursion will be independent of the spot size (*parallel to point focusing*).

   $$x(s) = \sqrt{\beta(s)\beta^\star}\theta^\star \tag{84}$$

   Imposing the condition that the measurement can only be made for a excursion larger than K (10-15) times the beam size we obtain an expression for the minimal scattering angle:

   $$x(s) = \sqrt{\beta(s)\beta^\star}\theta^\star_{\min} = K\sqrt{\beta(s)/\beta^\star}\sigma^\star \tag{85}$$

   $$\Rightarrow \quad \theta^\star_{\min} = K\frac{\sigma^\star}{\beta^\star} = K\Delta\theta^\star \tag{86}$$

The minimum measurable scattering angle is just K times the divergence of the beam at the interaction point. In order to observe processes with a small scattering angle, as for example elastic pp scattering, one needs an interaction region with a small beam divergence and, hence, high $\beta^\star$.

Measurements of the differential elastic cross-section $dN_{\rm el}/dt$ at small momentum transfer t can be used to measure the total hadronic cross section $\sigma_{\rm tot}$ [6]. The optical theorem relates the total hadronic cross-section to the forward elastic scattering rate:

$$\sigma_{\rm tot}{}^2 = \frac{1}{\mathcal{L}} \frac{16\pi(\hbar c)^2}{1+\rho^2} \left. \frac{dN_{\rm el}}{dt} \right|_{t=0} \tag{87}$$

where $t = p^2\theta^2$ and

$$\rho = \frac{\Re F(s, t=0)}{\Im F(s, t=0)} \tag{88}$$

$F(s, t=0)$: Elastic forward scattering amplitude. Using the relation

$$\sigma_{\rm tot} = \frac{N_{\rm el} + N_{\rm inel}}{\mathcal{L}} \tag{89}$$

the luminosity $\mathcal{L}$ can be eliminated and one can express the total hadronic cross section as a function of the interaction rate $N_{\rm el} + N_{\rm inel}$ and the forward scattering rate:

$$\sigma_{\rm tot} = \frac{16\pi(\hbar c)^2}{1+\rho^2} \frac{\left. \frac{dN_{\rm el}}{dt} \right|_{t=0}}{N_{\rm el} + N_{\rm inel}} \, . \tag{90}$$

References

[1] P.J. Bryant and K. Johnson, 'The Principles of Circular Accelerators and Storage Rings', Cambridge University Press. (1992).

[2] E.D. Courant, M.S. Livingston and H.S. Snyder, Phys. Rev. **88**, (1952) 1190-6.
E.D. Courant and H.S. Snyder, Annals of Physics **3**, (1958), 1-48.

[3] P. Schmuser, 'Basic Course on Accelerator Optics', CERN 87-10 (1987) 1-44.

[4] K.G. Steffen, 'High Energy Beam Optics', Interscience Publishing, New York, Wiley and Sons (1965)

[5] J. Buon, 'Beam Phase Space and Emittance', CERN 94-01 (1994) 89-115.

[6] U. Amaldi in 'Laws of Hadronic Matter', Ed. A. Zichichi (1975) 673.

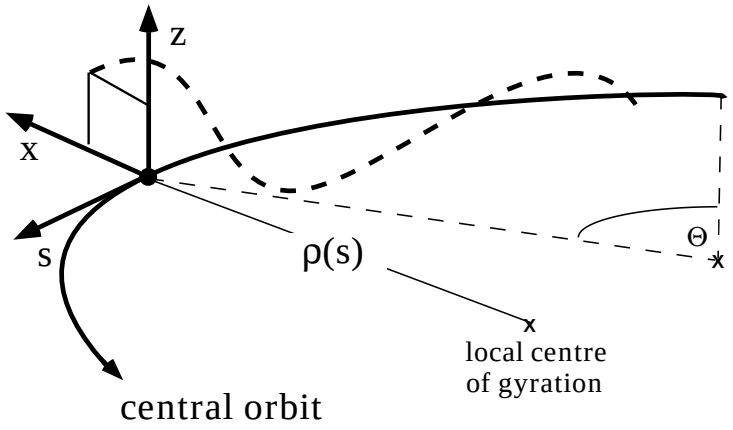

Figure 1: *Coordinate System*

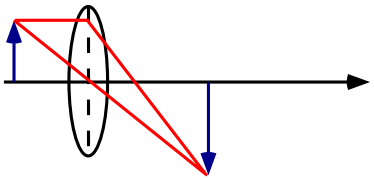

Figure 2: *Ray Optical Construction of an Image*

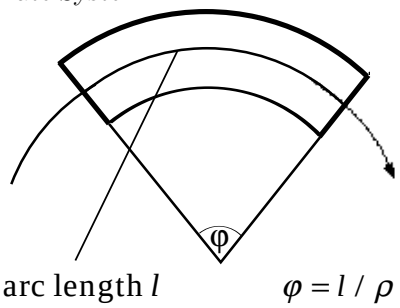

Figure 3: *Sector Dipole Magnet*

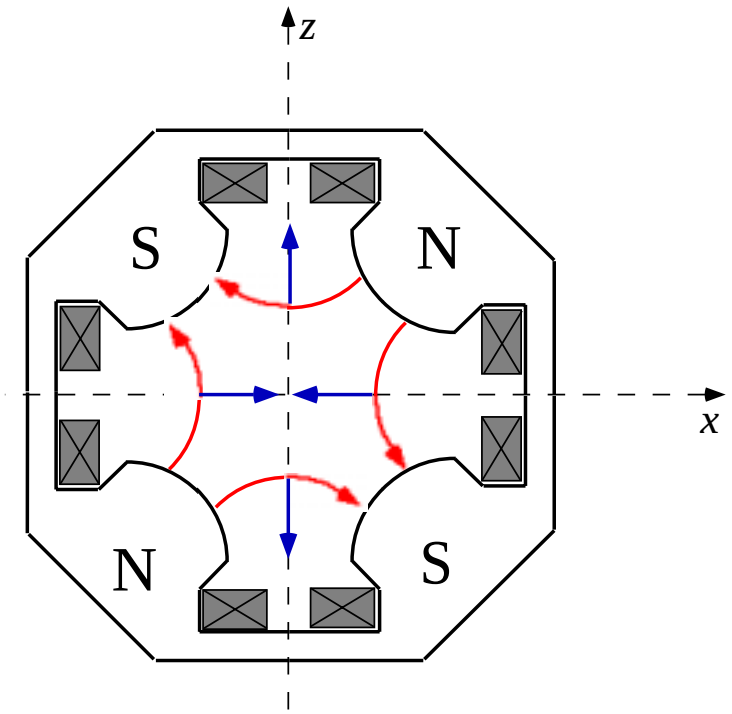

Figure 4: *Quadrupole Magnet*

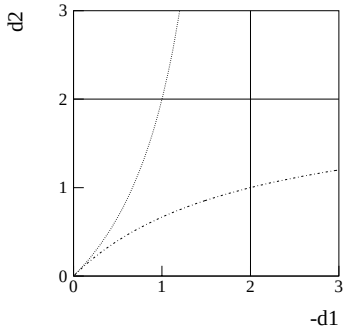

Figure 5: *Necktie Diagram*

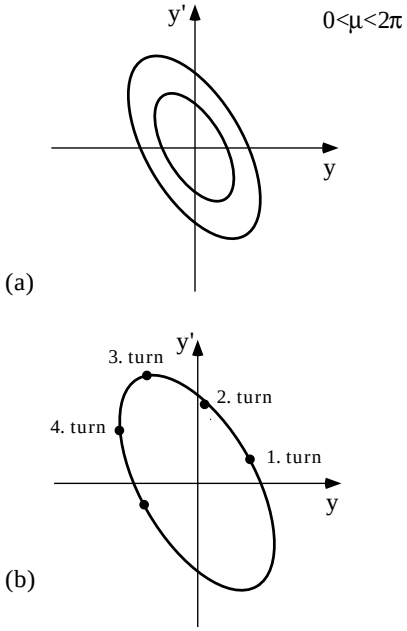

Figure 6: *Phase Space Ellipses*

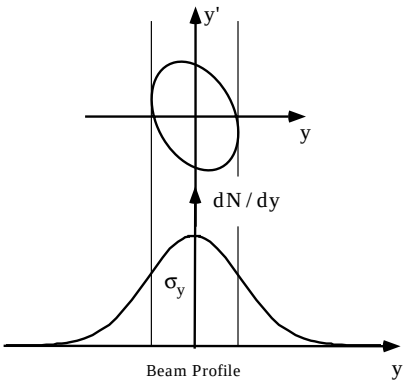

Figure 7: *Beam Profile*

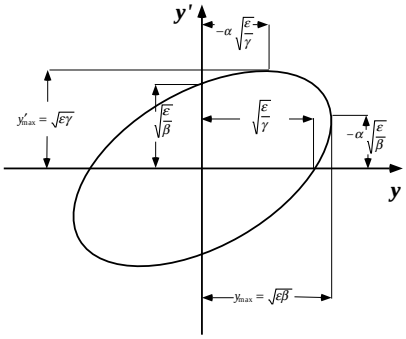

Figure 8: *Beam Parameters*

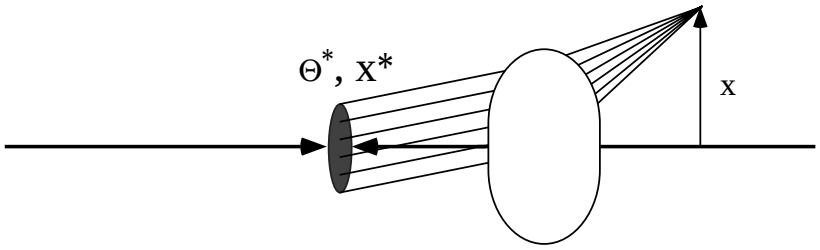

Figure 9: *Parallel to Point Focusing*

4 Imperfections and Resonances

So far we learned that free particle motions relative to the nominal orbit of a circular accelerator can be described by the β-function. The particles oscillate in a pseudo harmonic manner. We will see in the following, that using the known β-function the particle co-ordinates can be renormalized such that the motion is harmonic in the new system. From our knowledge about forced harmonic oscillations we gain insight in the perturbed particle motion of a circular accelerator [1].

Consider the inhomogeneous Hill Equation

$$\frac{d^2}{ds^2}x(s) + K(s)x(s) = f(s)\,. \tag{1}$$

The inhomogeneity $f(s)$ may describe any perturbation like magnetic dipole and quadrupole field errors or a momentum deviation. Inserting the pseudo harmonic ansatz from the previous chapter one obtains a non-linear differential equation for $\beta(s)$

$$\frac{d^2}{ds^2}\beta^{\frac{1}{2}} + K(s)\beta^{\frac{1}{2}} = \beta^{-\frac{3}{2}}\,. \tag{2}$$

The equation can be simplified by introducing new variables η and ϕ:

$$\eta = \frac{x}{\sqrt{\beta}} \;\text{ and }\; d\phi = \frac{ds}{Q\beta} \qquad (\textit{Floquet Transformation}) \tag{3}$$

Inserting the new variables into equ. (1) yields:

$$\frac{d^2}{d\phi}\eta + Q^2\eta = \frac{\beta^{\frac{3}{2}}}{Q^2}f(\phi)\,, \tag{4}$$

which is the equation of motion for a forced harmonic oscillator with driving term $\beta^{3/2}/Q^2 f(\phi)$. For free oscillations the solution is

$$\eta(\phi) = \eta_0 \sin Q(\phi - \phi_0)\,. \tag{5}$$

Before discussing the general solutions let us recall what we know about the forced harmonic oscillator.

4.1 Forced Harmonic Oscillator

The equation of motion of a free harmonic oscillator is:

$$\ddot{x}(t) + \omega_0^2 x(t) = 0\,. \tag{6}$$

Its solution can be written in the form

$$x(t) = a \sin(\omega_0 t + \varphi) \tag{7}$$

In case the oscillations are driven by a time dependent force $f(t)$ the equation of motion is

$$\ddot{x}(t) + \omega_0^2 x(t) = \frac{f(t)}{m} \tag{8}$$

A general solution of the inhomogeneous diff. equation can be found using the so called retarded Green's Function $G(t|t_0)$ which is defined as the response of the system to a δ-pulse at $t = t_0$:

$$\ddot{G}(t|t_0) + \omega_0^2 G(t|t_0) = \frac{\delta(t - t_0)}{m} \tag{9}$$

which is:

$$G(t - t_0) = \frac{1}{m} \frac{\sin \omega_0 (t - t_0)}{\omega_0} \theta(t - t_0) \tag{10}$$

The general solution is then obtained by time convolution of the retarded Green's Function with the driving term $f(t)$:

$$x(t) = \frac{1}{m\omega_0} \int_{-\infty}^{t} \sin \omega_0 (t - t_0) f(t_0) dt_0 \,. \tag{11}$$

If the driving term is periodic in time with period T

$$f(t_0 + T) = f(t_0) \Rightarrow x(t_0 + T) = x(t_0) \,, \tag{12}$$

as it is the case for the most important perturbations in a circular accelerator, the solution can be written in the form

$$m\omega_0 x(t) = \frac{1}{2 \sin \frac{\omega_0 T}{2}} \int_{t}^{t+T} \cos \left[\omega_0 (t - t_0) + \frac{\omega_0 T}{2} \right] f(t_0) dt_0 \tag{13}$$

4.2 The Inhomogeneous Hill Equation

Now let us apply what we learned from the forced harmonic oscillator to the inhomogeneous Hill Equation.

$$\frac{d^2\eta}{d\phi^2} + Q^2 \eta = f(\phi) \text{ with } \; f(\phi) = Q^2 \beta^{3/2} f(s) \tag{14}$$

Assuming that the perturbation has a periodicity $\Delta\Phi = 2\pi$ the solution is:

$$\eta(\phi) = \frac{1}{2 \sin \pi Q} \int_{\phi}^{\phi + 2\pi} \cos \left[Q(\phi_0 - \phi) - \pi Q \right] g(\phi_0) d\phi_0 \tag{15}$$

In real space and time it can be re-expressed as:

$$x(s) = \frac{\sqrt{\beta(s)}}{2\sin\pi Q}\int_s^{s+C}\sqrt{\beta(t)}\cos\left[Q(\phi(t)-\phi(s))-\pi Q\right]f(t)dt \tag{16}$$

being equivalent to

$$x(s) = \frac{\sqrt{\beta(s)}}{2\sin\pi Q}\int_0^{C}\sqrt{\beta}(t)\cos\left[|Q(\phi(t)-\phi(s)|-\pi Q\right]f(t)dt \tag{17}$$

The latter expression is more convenient if the convolution integral is calculated on a computer.

4.3 Solution in Frequency Space

Since the excitations are periodic in time it is for many applications useful to consider the solution of the inhomogeneous Hill equation in frequency space. We replace the driving term by its Fourier decomposition:

$$\frac{d^2\eta}{d\phi^2} + Q^2\eta = g(\phi) = \sum_k f_k e^{ik\phi}, \tag{18}$$

with the Fourier coefficients

$$f_k = \frac{1}{2\pi}\int_0^{2\pi} g(\phi)e^{-ik\phi}d\phi \tag{19}$$

In frequency space the Hill equation transforms into

$$-\omega^2\hat{\eta} + Q^2\hat{\eta} = \hat{g}(\omega) \tag{20}$$

for which we find the solution

$$\hat{\eta} = \frac{\hat{g}(\omega)}{Q^2-\omega^2} \tag{21}$$

Transforming back into the η-space one obtains

$$\eta = \int_0^{2\pi} e^{i\omega\phi}\frac{\hat{g}(\omega)}{Q^2-\omega^2}d\omega = \int_0^{2\pi} e^{i\omega\phi}\frac{\sum_k f_k e^{ik\phi}\delta(k-\omega)}{Q^2-\omega^2}d\omega = \sum_k \frac{f_k}{Q^2-k^2}e^{ik\phi} \tag{22}$$

Interpretation:

1. The closed orbit becomes unstable as the tune Q of the machine approaches an integer value ($Q = 1,\ 2,\ 3\ \ldots$).

2. For a given perturbation the distortion of the motion is proportional to $\sqrt{\beta}$. Thus high β positions are ideal for beam position monitors and orbit correctors (dipole kicks). On the other hand, the quadrupoles of a low-β insertion the β-value can reach very high values (~ 4000 m at LHC). These quadrupoles must be very accurately aligned and the field quality must be very good to guarantee a stable particle motion.

4.4 Particle Motion with Momentum Deviation: Dispersion

In the derivation of the Hill equation we already took into account that the particle has a small momentum deviation Δp with respect to the nominal momentum p_0. In this case the equation of motion is

$$x''(s) + K(s)x(s) = \frac{1}{\rho(s)}\frac{\Delta p}{p_0}\,. \tag{23}$$

Obviously the excursion will be proportional to the relative momentum deviation $\Delta p/p_0$. To get rid of this trivial factor one defines the *dispersion function* D(s):

$$D(s) = \frac{x(s)}{\Delta p/p_0} \tag{24}$$

which is the solution of the differential equation

$$D''(s) + K(s)D(s) = \frac{1}{\rho(s)} \tag{25}$$

Inserting into equ. (17) the driving term $1/\rho(s)$ one obtains the solution:

$$D(s) = \frac{\sqrt{\beta(s)}}{2\sin(\pi Q)}\int_0^C \sqrt{\beta(t)}[|Q(\phi(t)-\phi(s))| - \pi Q]\frac{1}{\rho(t)}dt \tag{26}$$

Examples:

1. Beam Size Including the effect of the beam momentum spread the total beam size is given by:

$$\sigma_{\rm beam} = \sqrt{\epsilon\beta + (D\Delta p/p_0)^2} \tag{27}$$

2. Measurement of momentum deviations at the LHC

   In Fig. 1, we compare the excursion of a particle with $\Delta p/p_0 = 5\,10^{-3}$ to the 10σ beam profile of the LHC beam close to the interaction point ($s = 0$) [2]. We see that for $s > 300\,\mathrm{m}$ the excursion is larger than 10 times the beam with and special detectors can be used to measure the excursion of the particles.

   In case of the LHC one can measure particles with relative momentum deviations between $2\,10^{-3}$ and 0.1. One can envisage to use such measurements to study single diffractive scattering of protons. In this processes one proton is excited into a mass state X with mass M whereas the other stays intact but has a momentum deviation $\Delta p/p_0 = M^2/s$, where $\sqrt{s}$ is the center of mass energy.

3. Layout of a Low-β Insertion

   Low-β insertions are used to perform particle collisions at high luminosity. The general layout of such an insertion is sketched in Fig. 2. Two sets of quadrupoles are used to focus the β to a minimum value at the interaction point: the inner triplet (objective) and the outer triplet (ocular). The β function rises steeply behind the interaction point and reaches its maximum value within the inner triplet. The outer triplet is followed by a sequence of quadrupoles and dipoles which is tuned such that the dispersion is zero at the interaction point and the contribution of the momentum spread to the beam spot size vanishes. Dipoles close to the interaction point are used to cross and separate the colliding beams.

4. Tidal Forces and the LEP beam energy

   The momentum compactation α of a circular accelerator or storage ring relates the momentum deviation Δp of a particle to the increase ΔC of the orbit length

$$\alpha = \frac{\Delta C/C_0}{\Delta p/p_0} \,. \tag{28}$$

   Inversely, a change of the orbit length can be related to a momentum or energy change. Such changes of the orbit length are caused by tidal forces acting on the rocks into which the accelerator structure is embedded [3]. The time dependent gravity variation $\Delta g/g_0$ are related to the change of orbit length via the coefficient

$$\alpha_{\rm str} = \frac{\Delta C(t)/C_0}{\Delta g(t)/g_0} < 0 \tag{29}$$

   and using the momentum compactation the expected energy variations can be directly related to the gravity variations:

$$\frac{\Delta E(t)}{E_{\rm tide=0}} = -\frac{\alpha_{str}}{\alpha}\frac{\Delta g(t)}{g_0} \,. \tag{30}$$

   The results of such a measurement at the LEP together with the theory prediction are shown in Fig. 2.

4.5 Distortion from Dipole Kicks

The next perturbation we want to consider are deviation ΔB from the nominal dipole field B_0. The driving term $f(s)$ is now proportional to the field error distribution:

$$f(s) = \frac{1}{\rho(t)}\frac{\Delta B(t)}{B_0} \tag{31}$$

Inserting the driving term into equ. (17) one obtains the closed orbit solution:

$$x(s) = \frac{\sqrt{\beta(s)}}{2\sin\pi Q}\int_0^C \sqrt{\beta(t)}\cos\left[|Q(\phi(t)-\phi(s))|-\pi Q\right]\left(\frac{1}{\rho(t)}\frac{\Delta B(t)}{B_0}\right)dt \tag{32}$$

The simplest error distribution one can imagine is a 'single kick' at phase $\phi = \phi_0$ represented by a δ-pulse of the height $\Delta(B\ell)/B_0$. In this case the solution can be calculated analytically:

$$x(\phi) = \frac{\sqrt{\beta(\phi)\beta(\phi_0)}}{2\sin\pi Q}\frac{\Delta(B\ell)}{\rho(\phi_0)B_0}\cos\left[|Q(\beta(\phi_0)-\phi)|-\pi Q\right] \tag{33}$$

The response to a single dipole kick plotted in Fig. 3 is represented by two cosine-waves emerging from the point where the perturbation occurs. The strength of the response is proportional to the excitation and to $\sqrt{\beta}$ at the excitation point.

4.6 Quadrupole Errors and Second Order Resonances

As we saw in the previous section, dipole kicks cause particle oscillation with amplitudes proportional to the strength of the kick. The motion becomes unstable if the tune Q of the machine approaches integer values. A different kind of resonances occurs if the perturbations are caused by quadrupole errors. In this case not only the amplitude but also the phase of the motion is modulated.

To understand this we draw the phase space diagram for the perturbation at phase ϕ_0 (Fig. 4). The particle excursion is:

$$x = a\cos Q\phi_0 \tag{34}$$

The crucial point is that the kick caused by a quadrupole error $\Delta(kl)$ is proportional to the particle excursion

$$\Delta x' = \frac{\Delta(Bl)}{B\rho} = \frac{\Delta(kl)x}{B\rho} \tag{35}$$

Simple geometry shows that the amplitude change caused by the kick is

$$\Delta a = \beta_0\Delta x'\sin Q\phi_0 \tag{36}$$

and the phase shift is given by

$$2\pi\Delta Q = \frac{\beta_0\Delta x'}{a}\cos Q\phi_0 \tag{37}$$

Inserting the excursion and the strength of the kick one obtains for the tune shift:

$$\Delta Q = \frac{\beta_0\Delta(kl)}{4\pi B\rho}(\cos 2Q\phi_0 + 1) \tag{38}$$

As shown in Fig. 5, the quadrupole error induces a shift and a modulation of the tune of the machine. Note that the motion becomes unstable if the band covered by the modulation includes an integer Q value.

From Fig. 6, we see that a special situation occurs for half integer Q values. Since the strength of the excitation is proportional to the excursion it acts always in the same direction as the particle motion. For half-integer $Q-$values the amplitude changes add up coherently and the motion becomes unstable (second order resonances).

4.7 Third Order Resonances

The common feature of the responses to dipole and quadrupole kicks are that their strength does not depend of the particle amplitude itself. This situation changes if we consider sextupole errors. Here the kick is proportional to the square of the particle excursion:

$$\Delta B = \frac{d^2 B_z}{dx^2} x^2 = \frac{1}{2} B'' x^2 \tag{39}$$

$$\beta \Delta x' = \frac{\beta l B''}{2B\rho} x^2 = \frac{\beta l B''}{2B\rho} a^2 \cos Q\phi_0{}^2 \tag{40}$$

Using the same procedure as above one obtains for the change in amplitude:

$$\frac{\Delta a}{a} = \frac{\beta \ell B''}{8B\rho} \sin 3Q\phi \tag{41}$$

and for the phase shift:

$$2\pi \Delta Q = a \frac{\beta l B''}{8B\rho} \cos 3Q\phi \tag{42}$$

We see that the relative change of the amplitude $\Delta a/a$ and the tune shift are proportional to the amplitude a. The consequence is that stability of the motion is not only a matter of tune but also of the amplitude. Or more general, their are areas in the phase space plane where the motion is stable (small amplitudes) and areas where it is unstable (large amplitudes).

References

[1] E. Wilson, CERN 94-01 (1994) 131-158 and 239-251.

[2] K. Eggert and A. Morsch, Nucl. Instrum. Methods **A351** (1994) 174-182.

[3] L. Arnaudon *et al.* , CERN SL/94-71 (BI) (1994).

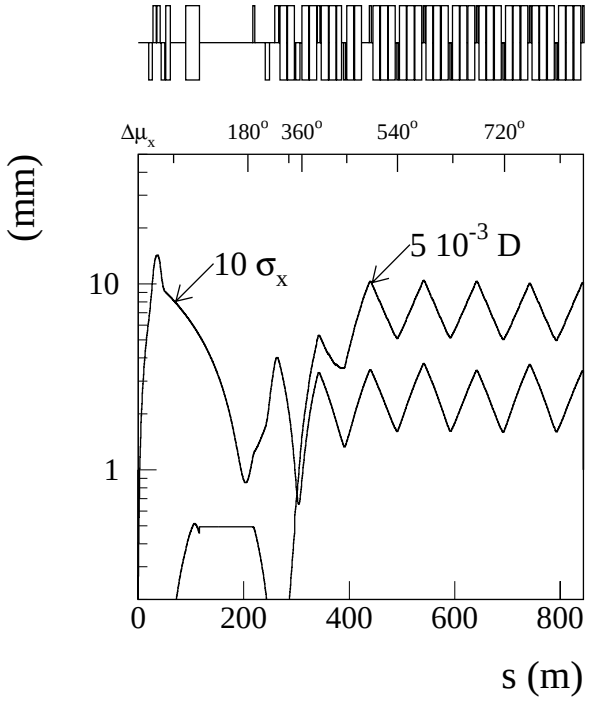

Figure 1: *Beam Profile and Dispersion in a LHC Intersection Region*

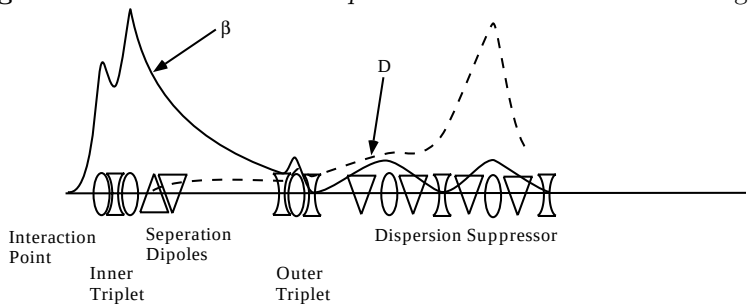

Figure 2: *Sketch of a low-β Insertion*

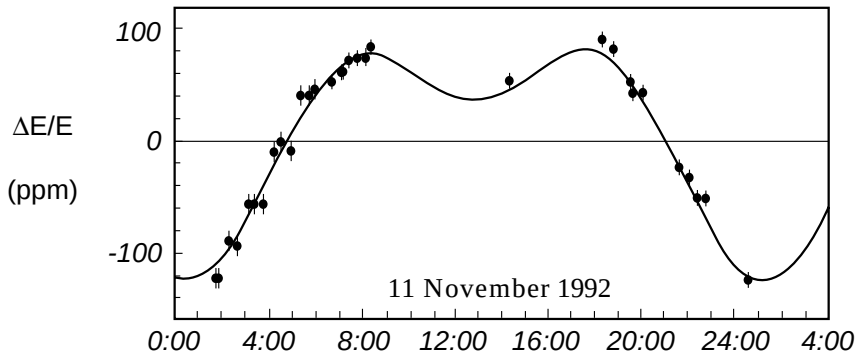

Figure 3: *Evolution of the relative LEP beam energy variation due to tides.*

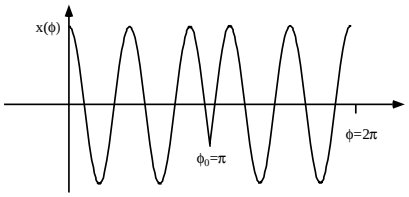

Figure 4: *Response to a Dipole Kick*

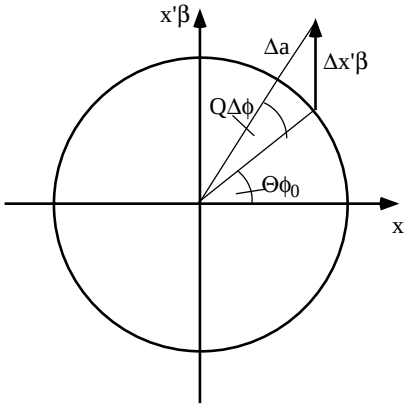

Figure 5: *Kick due to Quadrupole Error*

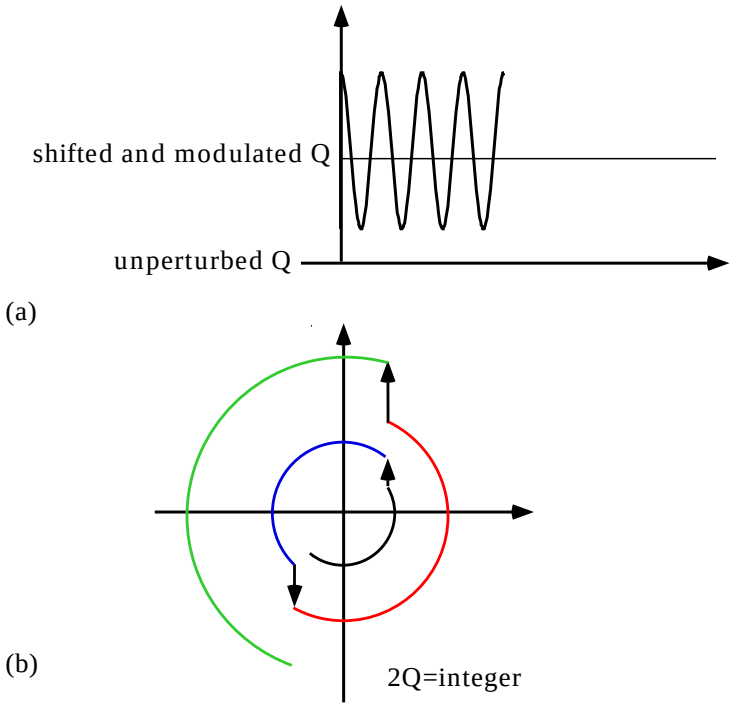

Figure 6: *(a) Stop Band (b) Half Integer Resonance*

5 Longitudinal Beam Dynamics

In this chapter we shortly treat the longitudinal motion of particles in circular machines. The variables in which the motion is usually described are the energy of the particle referred to the nominal energy and the phase difference referred to the nominal phase. We will see that the nominal phase difference with respect to accelerating electric RF field can be chosen such that the particles perform stable oscillations about this value (*synchrotron oscillations*). Refs. [1] and [2] were used to prepare this lecture and more details can be found there.

5.1 Maxwell Equation

Circular accelerators use time varying electro-magnetic fields to accelerate charged particles. The general expression for the force acting on a particle with charge q moving with the velocity $\vec{v}$ in an electric field $\vec{E}$ and a magnetic field $\vec{B}$ is:

$$\vec{F} = q\vec{E} + q(\vec{v} \times \vec{B})\,. \tag{1}$$

Only the component of the force parallel to $\vec{v}$ can increase the velocity of the particle. This component is proportional to $\vec{v}\vec{F}$

$$\vec{v}\vec{F} = e\vec{E}\vec{v} + e\underbrace{(\vec{v} \times \vec{B})\vec{v}}_{0}\,. \tag{2}$$

We see that the magnetic field cannot be used for acceleration. From Maxwell's Equation we know, however, that a time varying magnetic field induces an electric field. Let Φ and $\vec{A}$ be the magnetic and electric potentials, respectively. Then the electric field is given by:

$$\begin{array}{lll} \vec{E} = & -\vec{\nabla}\Phi & -\frac{\partial}{\partial t}\vec{A} \\ & \swarrow & \downarrow \\ \text{dc-acceleration} & & \vec{B} = \vec{\nabla} \times \vec{A} \\ & & \vec{\nabla} \times \vec{E} = -\frac{\partial}{\partial t}\vec{B} \end{array} \tag{3}$$

Electrostatic accelerators as for example the Van de Graaf accelerator make use of the first term. The second term offers two different solutions. This can be seen by rewriting it as an integral equation:

$$\oint_{\mathcal{C}} \vec{E}d\vec{s} = \iint_{\mathcal{S}} \vec{\nabla} \times \vec{E}d\vec{S} = -\frac{\partial}{\partial t}\iint_{\mathcal{S}} \vec{B}d\vec{S} \tag{4}$$

The two topological scenarios illustrated in Fig.1 are possible. Scenario (a) is realized in the *Betatron* and scenario (b) in circular machines using RF cavities.

5.2 Betatron Acceleration

In the betatron, a time varying magnetic field is used to accelerate the particles and to hold them on a constant circular orbit. The electric field at the particle orbit is related to the flux of the magnetic field through the circle inclosed by the particle by:

$$E_s - -\frac{1}{2\pi r}\frac{\partial}{\partial t}\iint_{\mathcal{S}} \vec{B} d\vec{S}\,. \tag{5}$$

The radius of the orbit has to be constant during acceleration, which leads to the relation:

$$\left.\begin{array}{l} \frac{d(mv)}{dt} = eE_s \\ mv = -eB_s r \end{array}\right\} r = const. \Rightarrow \frac{d(mv)}{dt} = eE_s = -er\frac{dB_s}{dt} \tag{6}$$

Insertion into equ. (5) gives:

$$2\frac{dB_s}{dt} = \frac{1}{\pi r^2}\frac{\partial}{\partial t}\iint_{\mathcal{S}} \vec{B} d\vec{S}\,. \tag{7}$$

The right side is just the rate of change of the magnetic field averaged over the circle area (B_{av}). Hence, the stability condition can be written as:

$$2\frac{dB_s}{dt} = \frac{dB_{av}}{dt} \quad \text{(Wideröe Condition)}\,. \tag{8}$$

5.3 Acceleration with Cavities

Let's assume that the circular accelerator has one acceleration gap to which a voltage with frequency $\omega(\tau)$ is applied. The condition that the particle stays in phase with the high frequency voltage is:

$$\int_0^t \omega(\tau)d\tau + h\Theta = const. \Leftrightarrow\ h\dot{\Theta} = \omega\,, \tag{9}$$

where $\theta = s/(2\pi\rho) = s/C_0$. This leads to the *synchrotron condition*:

$$\omega = h\Omega_0 = h\frac{2\pi v_0}{C_0}\,. \tag{10}$$

Hence, the frequency of the time varying electric field has to be an integer multiple h of the revolution frequency; h is called the *harmonic number*.

Since the particle beam has a certain momentum spread, the revolution frequencies and orbit lengths are different for each particle and hence, each particle will arrive at the acceleration gap at a different time experiencing an

acceleration different from that of the particle on the nominal orbit. To study the longitudinal motion we first write down the equation of motion:

$$\frac{d}{dt}p = \underbrace{\frac{e\hat{u}}{C}\cos\theta_0}_{\text{eff. traveling wave acceleration}} \quad \underbrace{-\frac{e}{C}\int_0^R 2\pi r \frac{\partial B}{\partial t} dr}_{\text{Ramping}} \; . \tag{11}$$

Here, $\hat{u}$ is the peak RF voltage, C_0 the orbit length and θ_0 the phase at which the nominal orbit arrives at the acceleration gap (Fig. 2). The force acting on the particle has two components: the first arises from the electric field in the cavity and the second is induced by the magnetic field, which has to be increased during acceleration in order to keep the particles on a constant orbit (*ramping*). We assume that the voltage is independent of the radial position and that the rate of change of the particle momentum is much smaller than the revolution frequency. The momentum deviation with respect to the nominal particle of a particle arriving at a phase θ is then given by the relation:

$$C\frac{d}{dt}p - C_0\frac{d}{dt}p_0 = e\hat{u}(\cos\theta - \cos\theta_0) - \int_{R_0}^{R} 2\pi r \frac{\partial B}{\partial t} dr \tag{12}$$

Applying the first order expansions $R = R_0 + \Delta R,\ C = C_0 + \Delta C,\ p = p_0 + \Delta p$ yields

$$\Delta C\frac{d}{dt}p_0 + C_0\frac{d}{dt}\Delta p = e\hat{u}(\cos\theta - \cos\theta_0) - eC_0\left(\frac{\partial B}{\partial t}\right)_0 \Delta R \; . \tag{13}$$

Inserting the *Cyclotron Relation* $p_0 = -eB_0R_0$ we see that the ramping term vanishes:

$$\frac{d}{dt}\Delta p = \frac{e\hat{u}}{C_0}(\cos(\theta_0 + \Delta\Theta) - \cos\theta_0) \; . \tag{14}$$

The differential equation for the longitudinal motion contains now two time varying variables Δp and $\Delta\theta$ which are not independent. First we relate the revolution frequency difference $\Delta\Omega$ to the momentum deviation.

$$\Omega = 2\pi v/C \tag{15}$$
$$\Delta\Omega/\Omega_0 = \Delta v/v_0 - \Delta C/C_0 \tag{16}$$
$$\Delta v/v_0 = \gamma^{-2}\Delta p/p_0 \text{ with } \gamma = m/m_0 \tag{17}$$
$$\Delta C/C_0 = \alpha\Delta p/p_0 \text{ with Momentum Compactation } \alpha \tag{18}$$
$$\Delta\Omega/\Omega_0 = \eta\Delta p/p_0 \text{ with } \eta = \gamma^{-2} - \alpha \tag{19}$$

The variable η describes the net result of to competing effects: The revolution frequency increases with velocity but at the same time the bending radius is increased leading to a decrease of the frequency.

Now the momentum deviation can be related to the phase shift $\Delta\theta$

$$\Delta p = \frac{p_0}{\eta}\frac{\Delta\Omega}{\Omega_0} = \frac{m_0\gamma C_0}{2\pi\eta}\frac{\Delta\dot{\theta}}{h}\,, \tag{20}$$

which inserted into the equation of motion yields:

$$\frac{d}{dt}\left(\frac{m_0\gamma C_0}{2\pi h\eta}\frac{d}{dt}\Delta\theta\right) = \frac{e\hat{u}}{C_0}(\cos(\theta_0+\Delta\theta)-\cos\theta_0) \tag{21}$$

or shorter

$$\Delta\ddot{\theta} + \frac{{\Omega_s}^2}{\sin\theta_0}(\cos\theta-\cos\theta_0) = 0\,, \tag{22}$$

where we used the definition of the *synchrotron oscillation frequency*:

$$\Omega_s^2 = \frac{2\pi h\eta e\hat{u}\sin\theta_0}{C_0^2\gamma m_0} \tag{23}$$

The meaning of the definition becomes clear if one considers only small phase shifts. In this case one can perform the expansion:

$$\cos(\theta_0+\Delta\theta) = \cos\theta_0 - \Delta\theta\sin\theta_0 + \mathcal{O}(\Delta\theta^2) \tag{24}$$

and the diff. equation for the time evolution of the phase shift is

$$\Delta\ddot{\theta} - \Omega_s^2\Delta\theta = 0\,. \tag{25}$$

For $\Omega_s^2 < 0$ the particles perform harmonic oscillations with frequency Ω_s and for $\Omega_s^2 > 0$ the motion is unstable. Note that the sign of Ω_s is the sign of $\eta\sin\theta_0$ and one obtains two stability regions (Fig. 2):

$$\text{Stability Condition:}\begin{cases} 0 < \theta_0 < \pi/2 & \text{for } \gamma < 1/\sqrt{\alpha} \\ 0 > \theta_0 < -\pi/2 & \text{for } \gamma > 1/\sqrt{\alpha} \end{cases} \tag{26}$$

5.4 Longitudinal Emittance

As for the transverse motion there exists an invariant of the motion which is for small amplitudes:

$$\Delta p^2 + \left(\frac{E_0 C_0}{2\pi ch\eta}\right)^2 \frac{\Omega_s^2}{sin\Theta_0}\Delta\Theta^2 = const._t \tag{27}$$

Consider the high energy limit, where $\eta = \alpha$ and $\Delta E = \Delta p$, $\Delta\tau = \frac{C_0}{2\pi ch}$. Furthermore, we are interested in a situation where the nominal particle is not

accelerated anymore ($\theta_0 = \pi/2$, *stationary bucket*). Then the invariant of the motion can be written as:

$$\Delta E^2 + \left(\frac{E_0 \Omega}{\alpha}\right)^2 \Delta\tau^2 = A^2 = const. \tag{28}$$

Equation (28) describes an ellipse with area πA^2 in ΔE-$\Delta\tau$ phase space. In a beam consisting of many particles each particle moves on its own phase space ellipse. The longitudinal beam emittance is a measure of the area which the beam occupies in the $E - \tau$ space:

$$\varepsilon_l = 4\pi \Delta\tau \Delta E \ . \tag{29}$$

Here, $\Delta\tau$ and ΔE are the *rms* values of the τ and E distributions centered at the nominal values τ_0 and E_0.

The length of a particle bunch is related to $\Delta\tau$ through

$$\sigma_s = c\Delta\tau \tag{30}$$

and the longitudinal emittance can be related to the bunch length and energy spread through:

$$\varepsilon_l = 4\pi \frac{\sigma_s}{c} \Delta E \ . \tag{31}$$

Example:
The longitudinal emittance of the LHC proton beam will amount to 2.5 eVs and the relative momentum spread will be 1.1 10^{-4}. Using equation (31) we obtain for the *rms* bunch length 7.5 cm.

References

[1] P.J. Bryant and K. Johnson, 'The Principles of Circular Accelerators and Storage Rings', Cambridge University Press (1992).

[2] J. Le Duff, CERN 94-01 (1994) 289-311.

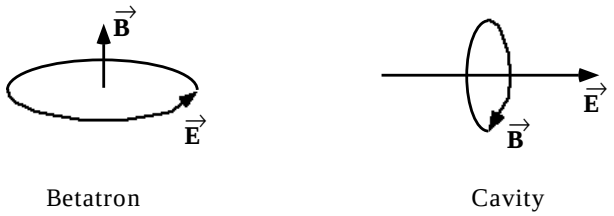

Figure 1: *Acceleration with Electro magnetic Fields*

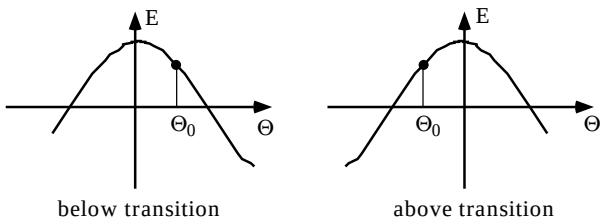

Figure 2: *Phase Stability*

6 Luminosity

6.1 Definition

The rate dR/dt at which we observe a particular reaction produced in the collision of two particle beams or the collision of a particle beam with a fixed target is equal to the reaction cross-section σ of the process times a quantity called Luminosity $\mathcal{L}$:

$$\frac{dN}{dR} = \sigma\mathcal{L} \tag{1}$$

The Luminosity is a measure for the density and overlap of the projectile and the target in the interaction region. It has to be defined in such a way that the interaction cross-section calculated from the interaction rate depends only on the types of the colliding particles and the center of mass energy $\sqrt{s}$ and not on the particle flux and the reference system. This guarantees that the cross-section becomes a quantity characterizing the underlying reaction process and which can be compared between experiments using different beams but work at the same $\sqrt{s}$.

In the case of a fixed target experiment the calculation of the luminosity is simplest [1] (Fig. 1). Assuming a homogeneous target medium with an front area much larger than the area A covered by the beam , the rate only depends on the flux of the incoming particles (i_{proj}), the particle density of the target medium (n_{tar}) and the length of the interaction region (l).

$$\frac{dR}{dt} = \sigma i_{\mathrm{proj}} n_{\mathrm{targ}} l \tag{2}$$

$$\mathcal{L} = i_{\mathrm{proj}} n_{\mathrm{targ}} l \tag{3}$$

We see that the unit of the luminosity is $\mathrm{cm}^{-2}\mathrm{s}^{-1}$. Assuming that in the fixed target scenario the beam has velocity $\beta_0 c$, the flux is $i = A\beta_0 c\gamma_0 n_{\mathrm{proj}}$.

Now we want to consider a system of colliding beams, which have velocities β_1 and β_2 and compare it to a fixed target scenario with the same $\sqrt{s}$ and target velocity β_0. In this case β_1 is not independent of β_2 but

$$\beta_1 = \frac{\beta_0 - \beta_2}{1 - \beta_0\beta_2} \tag{4}$$

The luminosity is now proportional to the product of the densities of the two beams times a relativistic flux factor β_{rel}.

$$\mathcal{L} \propto n_1 n_2 \beta_{\mathrm{rel}} \tag{5}$$

The flux factor can be obtained by applying the appropriate Lorentz-Transformation

into the corresponding fixed target system:

$$\begin{aligned} \beta_{\rm rel} n_1 n_2 &= \beta_{\rm rel}\gamma_1 n_{\rm proj}\gamma_2 n_{\rm tar} && (6)\\ &= \beta_0\gamma_0 n_{\rm proj} n_{\rm targ} && (7)\\ \Rightarrow & && (8)\\ \beta_{\rm rel} = \frac{\beta_0\gamma_0}{\gamma_1\gamma_2} &= \beta_1 + \beta_2 && (9) \end{aligned}$$

In a more general case, the two beams can cross under an arbitrary angle and the relativistic flux factor is:

$$\begin{aligned} \beta_{\rm rel} &= \sqrt{|\vec{\beta}_1 - \vec{\beta}_2|^2 - |\vec{\beta}_1 \times \vec{\beta}_2|^2} && (10)\\ &= \sqrt{\beta_1^2 + \beta_2^2 + 2\beta_1\beta_2\cos\phi - \beta_1^2\beta_2^2\sin\phi^2} && (11) \end{aligned}$$

Normally, one has to consider one of the following special cases

$$\beta_{\rm rel} = \begin{cases} 2\beta\cos\frac{\phi}{2}\sqrt{1-\beta^2\sin\frac{\phi}{2}^2} & \beta_1 = \beta_2 = \beta \\ \beta_{rel} = 2\cos\frac{\phi}{2}^2 & \beta = 1 \\ \beta_{rel} = 2 & \beta = 1, \;\; \phi = 0 \end{cases} \quad (12)$$

Before writing down the luminosity formula for arbitrarily shaped colliding beams we introduce some useful quantities describing the geometry of the beams.

6.2 Beam Profiles

Particles in storage rings travel in bunches or continuously (coasting beams), and collide either head-on or at a small angle ϕ. Mathematically, we can characterize the bunches by the *number of particles* per bunch (beam) N and the normalized *beam profile* (or density) $\rho(x, z, s, t)$. In the following we assume that there is no correlation between the three spatial coordinates and that the beam moves in the s-direction, x and z are the transverse directions:

$$\rho(\vec{r}; t) = \rho_x(x)\rho_z(z)\rho_s(s - ct) \quad (13)$$

$$\int_{-\infty}^{+\infty} dq\rho_q(q) = 1 \quad (q = x, y, z) \quad (14)$$

The x-axis is parallel to the crossing plane. The crossing is described by the transformation

$$\begin{aligned} x &\rightarrow x\cos\frac{\phi}{2} - s\sin\frac{\phi}{2} && (15)\\ s &\rightarrow x\sin\frac{\phi}{2} + s\cos\frac{\phi}{2}\,. && (16) \end{aligned}$$

Since the lateral dimension of the bunches is usually orders of magnitude larger than the transversal, the transformation of s simplifies to

$$s \rightarrow s \cos \frac{\phi}{2} \,. \tag{17}$$

The correlation function (overlap function) between two beam profiles is defined by the convolution:

$$\tilde{\rho}_q^{1,2}(q) = \int_{-\infty}^{+\infty} dr \rho_q^1(r) \rho_q^2(r-q) \,. \tag{18}$$

The *effective beam size* is defined as the inverse of the correlation function at the origin

$$q_{eff} = \frac{1}{\rho_q^{1,2}(0)} \tag{19}$$

From the normalization condition one obtains the *'Van der Meer' Relation* for symmetric beams

$$\int_{-\infty}^{+\infty} dq \tilde{\rho}_q^{1,2}(q) = 1 \tag{20}$$

6.3 Luminosity for Arbitrarily Shaped Beams

In the general case, the luminosity $\mathcal{L}$ is given by the time averaged integral of the product of the beam densities in the interaction point over the interaction volume $\mathcal{V}$ times the relativistic flux factor [3]:

$$\mathcal{L} = c\beta_{rel} N_1 N_2 \frac{1}{t_{\text{rev}}} \int_0^{t_{\text{rev}}} dt \int_{\mathcal{V}} d^3\vec{r} \rho_1(\vec{r},t) \rho_2(\vec{r},t) \,. \tag{21}$$

In the high energy limit of beams colliding with the same velocity $\beta_1 = \beta_2 = 1$ we write:

$$\begin{aligned} \mathcal{L} =& 2N_1 N_2 f \cos \frac{\phi}{2}^2 \int ds_0 \iiint dx dz ds \rho_x^1(x \cos \frac{\phi}{2} - s \sin \frac{\phi}{2}) \rho_x^2(x \cos \frac{\phi}{2} + s \sin \frac{\phi}{2}) \\ & \bullet \, \rho_z^1(z) \rho_z^2(z) \rho_s^1(s \cos \frac{\phi}{2} - s_0) \rho_s^2(s \cos \frac{\phi}{2} + s_0) \\ & \text{, where } s_0 = ct \text{ and } f \text{ is the revolution frequency.} \end{aligned} \tag{22}$$

Performing step by step the integration yields:

$$\begin{aligned}\mathcal{L} =& \frac{2N_1N_2f\cos\frac{\phi}{2}}{z_{eff}}\iint dxds\rho_x^1(x\cos\frac{\phi}{2}-s\sin\frac{\phi}{2})\rho_x^2(x\cos\frac{\phi}{2}+s\sin\frac{\phi}{2}) \\ & \bullet\int ds_0\rho_s^1(s\cos\frac{\phi}{2}-s_0)\rho_s^2(s\ \cos\frac{\phi}{2}+s_0)\end{aligned} \tag{23}$$

$$\begin{aligned}=& \frac{2N_1N_2f\cos\frac{\phi}{2}^2}{z_{eff}}\iint dxds\rho_x^1(x\cos\frac{\phi}{2}-s\sin\frac{\phi}{2})\rho_x^2(x\cos\frac{\phi}{2}+s\sin\frac{\phi}{2})\tilde{\rho}_s^{1,2}(2s\ \cos\frac{\phi}{2}) \\ =& \frac{2N_1N_2f\cos\frac{\phi}{2}}{z_{eff}}\int ds\tilde{\rho}_x^{1,2}(2s\sin\frac{\phi}{2})\tilde{\rho}_s^{1,2}(2s\cos\frac{\phi}{2})\end{aligned}$$

For small and large angles one finds the following limiting cases:

$$\mathcal{L} = \begin{cases} \frac{N_1N_2f}{x_{eff}z_{eff}} & \phi = 0 \\ \\ \frac{N_1N_2f}{x_{eff}s_{eff}} & \phi = \pi \end{cases} \tag{24}$$

Examples

1. Continuous beams with crossing angle ϕ (as at the ISR):

$$\rho_s^1(s) = \rho_s^2(s) = \frac{1}{2\pi R} \tag{25}$$

$$\tilde{\rho}_s^{1,2}(s) = \frac{1}{2\pi R} \tag{26}$$

$$\mathcal{L}_{\rm dc} = \frac{N_1N_2f\cos\frac{\phi}{2}}{2\pi Rz_{eff}}\int ds\tilde{\rho}_z^{1,2}(s\sin\frac{\phi}{2}) = \frac{N_1N_2f}{2\pi Rz_{eff}\tan\frac{\phi}{2}} \tag{27}$$

$$= \frac{I_1I_2}{e^2cz_{eff}\tan\frac{\phi}{2}}\,, \tag{28}$$

where

$$I = Nef \text{ and } f = \frac{c}{2\pi R} \tag{29}$$

2. Bunched beams with crossing angle ϕ and Gaussian profiles (as at the LHC)

$$\rho_s^1(s) = \rho_s^2(s) = \frac{1}{\sqrt{2\pi}\sigma_s} exp\left(-\frac{s^2}{2\sigma_s^2}\right) \quad (30)$$

$$\tilde{\rho}_s^{1,2}(s) = \frac{1}{2\sqrt{\pi}\sigma_s} exp\left(-\frac{s^2}{4\sigma_s^2}\right) \quad (31)$$

and equivalently for $\rho_x(x)$ and $\rho_z(z)$ but with widths σ_x and σ_z.

For the luminosity per bunch one obtains:

$$\mathcal{L}_{bunch} = \frac{N_1 N_2 f}{x_{eff} z_{eff}} \frac{1}{\sqrt{1 + \left(\frac{\tan\frac{\phi}{2} s_{eff}}{x_{eff}}\right)^2}} \quad (32)$$

with $x_{eff} = 2\sqrt{\pi}\sigma_x$, $z_{eff} = 2\sqrt{\pi}\sigma_z$ and$s_{eff} = 2\sqrt{\pi}\sigma_s$.

6.4 Vertex Distribution

The luminosity is calculated by integrating over the reaction volume or in other words by integrating over the vertex distribution. For many applications the vertex distribution is of special interest, it can be calculated from the relation:

$$\mathcal{L} = \frac{N_1 N_2 f cos\frac{\phi}{2}}{z_{eff}} \int ds \frac{\partial \mathcal{V}}{\partial s}(s) \quad (33)$$

$$\frac{\partial \mathcal{V}}{\partial s}(s) = \tilde{\rho}_z^{1,2}(s \sin\frac{\phi}{2}) \tilde{\rho}_s^{1,2}(s \cos\frac{\phi}{2}) \quad (34)$$

In general the crossing angle is small and the bunch shapes are approximately equal. Hence, we may write

$$\rho_s^1(s) = \rho_s^2(s) = \rho(s) \quad (35)$$

$$s \sin(\phi) \approx 0, \;\; \cos(\phi) \approx 1 \quad (36)$$

In this case, one obtains for the width σ_{vertex} of the vertex distribution:

$$\langle s^2 \rangle = \frac{\int ds\, s^2 \tilde{\rho}_s^{1,2}(2s)}{\int ds \tilde{\rho}_s^{1,2}(2s)} = \frac{1}{2} \int ds\, s^2 \rho(s) = \frac{1}{2}\sigma_s^2 \quad (37)$$

$$\sigma_{\text{vertex}} = \sqrt{\langle s^2 \rangle} = \frac{1}{2}\sigma_s \quad (38)$$

We see that the width of the vertex distribution is a factor $\sqrt{2}$ smaller than the bunch size.

Examples

1. Bunched beams with Gaussian shape

   The vertex distributions is Gaussian with $\sigma_{\rm vertex} = \frac{1}{2}\sigma_s \frac{1}{\sqrt{1+\left(\frac{\phi\sigma_s}{2\sigma_z}\right)^2}}$

2. Continuous beams with Gaussian profile

   The vertex distribution is Gaussian with $\sigma_{\rm vertex} = \frac{1}{\sqrt{2}sin\frac{\phi}{2}}\sigma_x$

6.5 The Van der Meer Method for Luminosity Measurements

Simon van der Meer [2] found a simple method for measuring the luminosity:

Displace the beams by a distance x_0 and record the event rate as a function of the displacement. The effective beam size in the direction of the displacement is then given by the ratio of the integral of the rate curve and the rate at $x_0 = 0$.

Applying the formalism discussed in the preceding sections it is easy to understand that this method works.

Assuming that the colliding beams are not aligned in the $x-$and$z-$ directions we have to modify the luminosity formula using the following transformation:

$$x \rightarrow x + x_0 \tag{39}$$
$$z \rightarrow z + z_0 \tag{40}$$

The reaction rate R recorded at at (x_0, z_0) is

$$R(x_0, z_0) = R_0 \int ds \tilde{\rho}_x^{1,2}(2s\sin\phi/2 - x_0)\tilde{\rho}_z^{1,2}\tilde{\rho}_s^{1,2}(2s\cos\phi/2) \tag{41}$$

In general, R_0 depends also on the acceptance A of the detector and the cross-section σ_{part} of the observed process. The maximum rate is observed when the displacements are equal to zero.

$$R(0,0) = R_0 \frac{1}{z_{eff}x_{eff}(s_{eff}, \phi)} \tag{42}$$

Integrating over the rate as a function of the displacements one obtains using the the *Van der Meer Relation* :

$$\int dx_0 R(x_0, 0) = R_0 \frac{1}{z_{eff}} \tag{43}$$

$$\int dz_0 R(0, z_0) = R_0 \frac{1}{x_{eff}(s_{eff}, \phi)} \tag{44}$$

The ratios of the integrals and the maximum value of the rate yield the effective beam sizes:

$$\frac{\int dz_0 R(0, z_0)}{R(0, 0)} = z_{eff} \tag{45}$$

$$\frac{\int dx_0 R(x_0, 0)}{R(0, 0)} = x_{eff}(s_{eff}, \phi) \tag{46}$$

The luminosity can now be calculated from the effective beam sizes and the beam currents using

$$\mathcal{L} = \frac{I_1 I_2}{e^2 f} \frac{1}{z_{eff} x_{eff}(s_e ff, \phi)} \,. \tag{47}$$

References

[1] K. Potter, CERN 94-01 (1994) 117-129.

[2] S. van der Meer, CERN/ISR 68-31 (PO) (1968).

[3] G. Guignard, CERN/ISR 77-10 (RD) (1977).

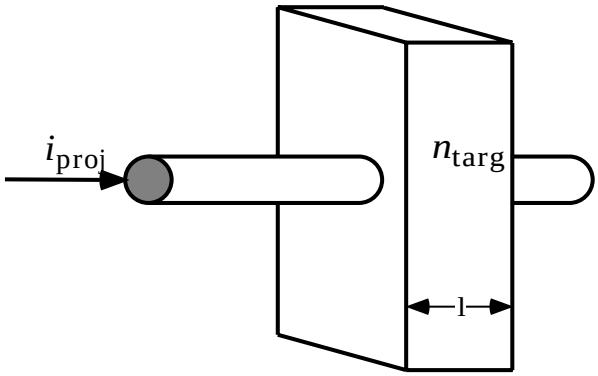

Figure 1: *Luminosity for a Fixed Target Experiment*